New naturally occurring mineral phases from the Krásno – Horní Slavkov area, western Bohemia, Czech Republic

Nové minerální fáze z oblasti Krásno – Horní Slavkov, západní Čechy, Česká republika

(43 figs, 21 tabs)

JIŘÍ SEJKORA[1] – RADEK ŠKODA[2] – PETR ONDRUŠ[3]

[1] *Department of Mineralogy and Petrology, National Museum, Václavské nám. 68, CZ-115 79 Prague 1, Czech Republic*
[2] *Institute of Earth Sciences, Faculty of Science, Masaryk University, Kotlářská 2, CZ-611 37, Brno, Czech Republic*
[3] *Biskupský dvůr 2, CZ-110 00 Prague 1, Czech Republic*

This paper presents description of eleven phases – probably new mineral species – from Krásno – Horní Slavkov, western Bohemia, Czech Republic. The phases characterized are mainly supergene phosphates. All up-to-now available physical and chemical data for individual phases and references to appropriate literature are given.

Key words: new natural phases; supergene minerals; phosphates; Krásno; Horní Slavkov; Czech Republic

Introduction

In the course of the prolonged study of mineralization in the Horní Slavkov – Krásno ore district, presented in this issue of the Journal (Beran – Sejkora, 2006; Plášil *et al*. 2006; Sejkora *et al*. 2006a, b, c), eleven new mineral phases have been encountered. This contribution presents the results of study of these phases.

The potentially new minerals are designated by symbols ***UNK1*** to ***UNK11***, derived from the words unnamed mineral Krásno and number of the phase. Individual phases are characterized to a variable degree, depending mainly on the type and quantity of material available for the study.

Methods of mineral identification

The surface morphology of samples was studied with the optical microscope Nikon SMZ1500 in combination with attached digital camera Nikon DXM1200F, used for photography in incandescent light. Scanning electron microscopes Tesla BS 340 (J. Sejkora and A. Gabašová; Czech Geological Survey, Prague) and JEOL JSM-6380 (J. Sejkora and J. Plášil, Faculty of Science, Charles University, Prague) were used to image surface details of the samples.

If not stated otherwise, all minerals described in this paper were identified by X-ray powder diffraction analysis. To minimize complicated shape of background due to classic glass sample holder, the samples studied were placed on the surface of a flat silicon wafer from suspension in ethanol. Step-scanned powder diffraction data were collected using the following instruments: Philips X'Pert MPD diffractometer (Czech Geological Survey, Prague) with a metallo-ceramic copper tube was operated at high-voltage of 40 kV and tube current of 40 mA; HZG4-AREM/Seifert diffractometer (National Museum, Prague) with a copper tube was operated at high-voltage 50 kV and tube current of 40 mA; and PANalytical X'Pert Pro diffractometer (Faculty of Science, Charles University, Prague) with X'Celerator detector, with secondary monochromator, using CuKα radiation at 40 kV and 30 mA.

The results were processed using X-ray analysis software ZDS for DOS (Ondruš 1993), Bede ZDS Search/Match ver. 4.5 (Ondruš – Skála 1997); unit-cell parameters were refined by program of Burnham (1962) and by program FullProf (Rodríguez-Carvajal 2005).

Quantitative chemical data were collected with the electron microprobe Cameca SX 100 (J. Sejkora and R. Škoda, Joint laboratory of Masaryk University and Czech Geological Survey, Brno). Studied samples were mounted in the epoxy resin discs and polished. The polished surfaces were coated with carbon layer 250 Å thick. Wavelength dispersion mode and operating voltage of 15 kV were used in all analyses. The beam current and diameter were adjusted to maintain stability of analyzed phases under the electron beam. Stable phases were analyzed using 20 nA current and 2 μm beam diameter. Less stable and highly hydrated minerals were analyzed using 10–4 nA and 10–30 μm beam diameter. For smaller aggregates (< 10 μm) of unstable minerals the beam diameter was as large as possible and the applied beam current was only 1–2 nA. The sequence of analyzed elements was adjusted to particular composition of the analyzed mineral. Volatile and major elements were analyzed first, followed by stable, minor and trace elements. Elevated analytic totals of minerals containing a large amount of hydroxyl group or crystalline water are generally caused by two factors: a) water evaporation under high vacuum conditions, well documented by collapsed crystals; b) water evaporation due to heating of the analyzed spot by electron beam. The dehydrated domain is seen as a notably brighter spot in backscattered electron images. Lower analytical totals for some samples are primarily caused by their porous nature or by poorly polished surface of soft or cryptocrystalline minerals.

In order to minimize peak overlap the following analytic lines and crystals were selected: Kα lines: F (PC1,

fluorapatite/topaz), Mg (TAP, forsterite), Na (TAP, albite), Al (TAP, sanidine), As (TAP, InAs), Si (TAP, sanidine), Cu (TAP, dioptase), K (PET, sanidine), P (PET, fluorapatite) Ca (PET, andradite), S (PET, barite), Ti (PET, TiO), Cl (PET, vanadinite), Fe (LIF, andradite), Mn (LIF, rhodonite), Ni (LIF, NiO), Zn (LIF, ZnO); Lα lines: Y (TAP, YAG), Sr (PET, $SrSO_4$), La (PET, LaB_6), Ce (PET, $CeAl_2$), Sm (LIF, SmF_3); Lß lines: Ba (PET, benitoite), Pr (LIF, PrF_3), Nd (LIF, NdF_3); Mα lines: Th (PET, ThO_2), Pb (PET, vanadinite); Mß lines: Bi (PET, metallic Bi), U (PET, metallic U). Peak counting times (CT) were 10 to 20 s for main elements and 30 to 60 s for minor and trace elements. CT for each background was ½ of peak time. In case that background was measured only one side of the peak, the counting time was the same as counting on the peak. As far as possible, elements present in minor and trace abundances were measured with highly sensitive crystals LPET a LLIF. Raw intensities were converted to the concentrations using automatic PAP (Pouchou – Pichoir 1985) matrix correction software package.

In analysis of some studied phases, accurate determination of fluorine content is important. Where possible, determination of fluorine was verified by measuring peak area (integrated intensity). This check was done irrespective of the note by Raudsep (1995) that with multilayer crystal monochromators (PC1) the effect of matrix is minimal. Fluorine contents measured by the two methods are practically identical.

Review of identified mineral phases

UNK1 CaAl silicate phosphate fluoride – $(Ca,Sr)_3Al_7(SiO_4)_3(PO_4)_4(F,OH)_3 \cdot 16.5\ H_2O$

UNK1 has been found in several samples collected in the Huber open pit. It is confined to cavities in strongly altered phosphate aggregates (Sejkora *et al.* 2006c), where it belongs to the youngest minerals. Such phosphate accumulations, ranging from 1 cm to 10 cm in size and sometimes accompanied by grains of unaltered green fluorapatite up to several cm long, are deposited in compact quartz. Triplite in these aggregates is almost completely replaced by compact pink-brown fluorapatite and isokite. Also accumulations to 2 by 3.5 cm composed dominantly of ***UNK1*** were observed, accompanied by whitish fluorapatite. The phase ***UNK1*** is accompanied by imperfectly shaped crystals of white and light yellow fluorapatite and rare zoned aggregates of F-rich crandallite, whitish crystals of kolbeckite and whitish earthy aggregates of the younger generation of isokite.

UNK1 forms compact and finely crystalline aggregates of chalk-white colour. This material, together with fluorapatite forms alteration products after the primary phosphate aggregates (Fig. 1). Cavities in these masses carry semi-spherical aggregates of ***UNK1*** to 0.1 mm with pearly lustre. The same phase forms rich crystalline aggregates deposited on light pink fluorapatite. These ag-

Fig. 1 White aggregates of ***UNK1*** with admixture of fluorapatite in cavity of aggregate of the primary phosphate. Huber open pit, Krásno. Width of the area shown 4.5 mm. Nikon SMZ1500, photograph by J. Sejkora.

gregates of ***UNK1*** are whitish with a weak yellow or green shade, partly transparent with a greasy lustre. Individual tabular crystals composing the aggregates are about 0.1 mm long (Fig. 2). Probably the most common are irregular, snow-white aggregates with pearly lustre, deposited in cavities in relict fluorapatite. Such aggregates grade to spheroidal aggregates (Fig. 3) composed of thin platy crystals (Fig. 4) up to 0.1 mm in size (Fig. 5).

Additional two different mineral assemblages host ***UNK1***. It crystallized as the youngest phase deposited on crystalline aggregates of UNK3 and kolbeckite, together with minerals of the chalcosiderite – turquoise series and pharmacosiderite. The second of the associations includes light yellow to buff crusts up to 3 mm thick, deposited on 1 cm long fluellite crystals, which in turn are sitting on milky-coloured fluorapatite in a cavity of quartz gangue.

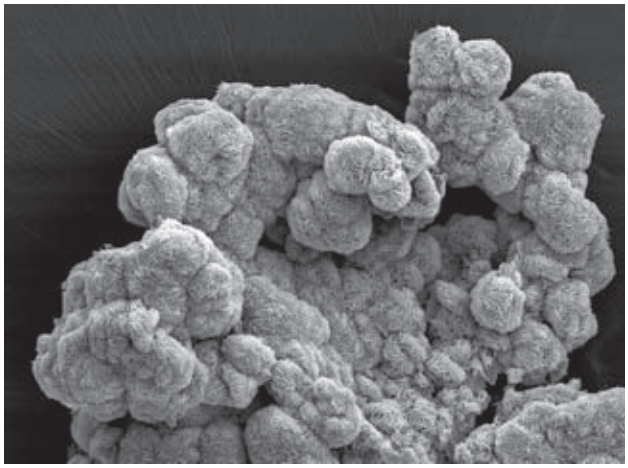

Fig. 3 Semi-spherical aggregates of ***UNK1***, Krásno. Width of the area shown 600 μm. SEM photograph Jeol JSM-6380, J. Sejkora and J. Plášil.

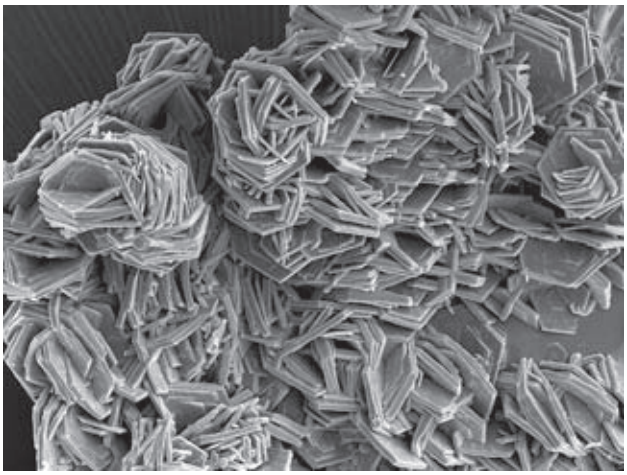

Fig. 2 ***UNK1*** aggregates composed of tabular crystals, Krásno. Width of the area shown 320 μm. SEM photograph Jeol JSM-6380, J. Sejkora and J. Plášil.

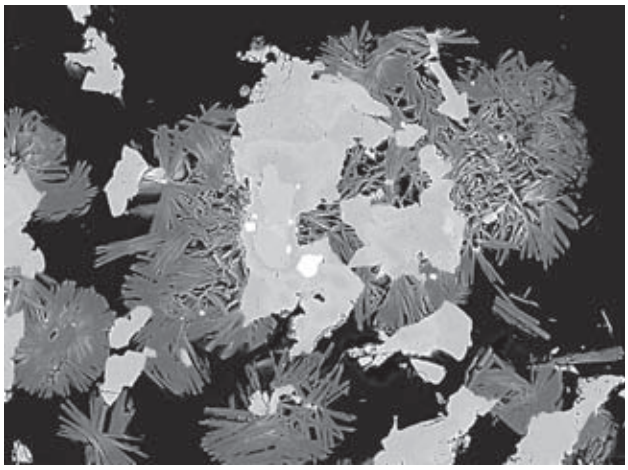

Fig. 4 Semi-spherical aggregates of ***UNK1*** composed of thin tabular crystals (dark grey), deposited on fluorapatite and other phosphates (light grey). Width of the area shown 400 μm BSE photograph, Cameca SX100, by J. Sejkora and R. Škoda.

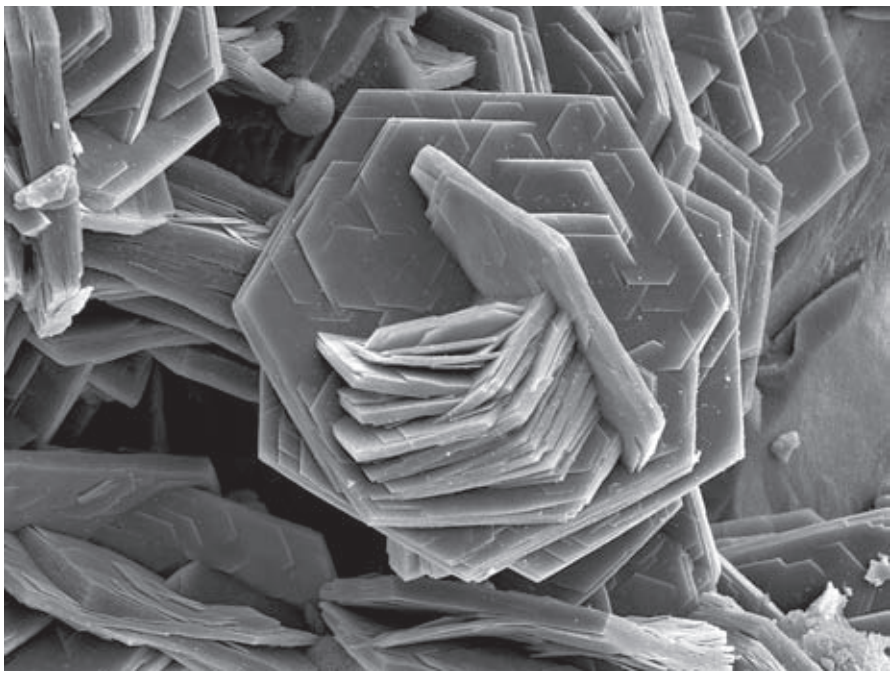

Fig. 5 Detail of tabular crystals of ***UNK1***, Krásno. Width of the area shown 80 μm. SEM photograph Jeol JSM-6380, J. Sejkora and J. Plášil.

The X-ray powder data for ***UNK1*** (Table 1) are close to data published for perhamite (Dunn – Appleman 1977). Besides differences in diffraction intensities, caused probably by preferred orientation of sample and instrumental differences, the most important difference is in the presence of an intense diffraction maximum with *d*-spacing of 20.2 Å. Refined unit-cell parameters of ***UNK1*** are close to those of perhamite (Table 2).

Table 2 Unit-cell parameters of ***UNK1*** (for hexagonal space group *P6/mmm*)

	UNK1 Krásno this paper	perhamite Newry Hill Dunn – Appleman (1977)
a [Å]	6.9939(6)	7.022(1)
c [Å]	20.200(2)	20.182(5)
V [Å^3]	855.7(1)	861.8

Table 1 X-ray powder diffraction pattern of ***UNK1***

$I_{rel.}$	*d*	*h*	*k*	*l*	$I_{rel.}$*	*d**	I_{rel}	*d*	*h*	*k*	*l*	$I_{rel.}$*	*d**
97	20.186	0	0	1			15	1.992	2	1	5	6	1.996
23	10.100	0	0	2	13	10.12	56	1.934	3	0	3	35	1.942
100	6.736	0	0	3	35	6.71	18	1.916	1	0	10	4	1.916
47	6.051	1	0	0	50	6.08	30	1.875	3	0	4	35	1.881
67	5.800	1	0	1	71	5.80	55	1.835	0	0	11	6	1.834
20	5.190	1	0	2	13	5.21	15	1.806	3	0	5	6	1.811
37	5.047	0	0	4	4	5.04	64	1.748	2	2	0	50	1.757
15	4.043	0	0	5			15	1.681	2	0	10	9	1.684
15	3.872	1	0	4	6	3.889	49	1.655	3	0	7		
60	3.496	1	1	0	50	3.510	11	1.603	2	1	9	9	1.604
27	3.361	0	0	6	9	3.369	7	1.5520	2	2	6	3	1.5551
57	3.103	1	1	3	50	3.115	17	1.5173	1	1	12	13	1.5165
41	2.994	2	0	1	35	3.005	7	1.5041	1	0	13	6	1.5003
56	2.942	1	0	6	35	2.947	1	1.4965	4	0	2	6	1.4831
50	2.900	2	0	2			12	1.4957	2	2	7		
87	2.873	1	1	4	100	2.882	51	1.4710	2	0	12	18	1.4715
73	2.763	2	0	3	25	2.773	10	1.4374	2	2	8	3	1.4219
33	2.644	1	1	5	25	2.650	6	1.3985	3	1	8		
36	2.605	1	0	7	13	2.606	30	1.3824	2	0	13	13	1.3837
59	2.524	0	0	8	18	2.524	12	1.3584	3	0	11		
25	2.425	1	1	6	25	2.429	4	1.3450	3	1	9	4	1.3483
48	2.330	1	0	8	9	2.330	11	1.3223	2	2	10	6	1.3272
8	2.286	2	1	0			8	1.2933	3	0	12		
51	2.250	2	0	6	25	2.252	7	1.2792	4	1	4		
15	2.231	2	1	2			9	1.2316	3	0	13		
21	2.168	2	1	3	18	2.175	11	1.2178	3	2	8		
75	2.104	1	0	9	35	2.104	5	1.1888	0	0	17		
20	2.048	1	1	8	6	2.052	9	1.1818	3	2	9		
10	2.018	3	0	0			11	1.1661	1	0	17		

$I_{rel.}$* and ***d**** – X-ray powder data of perhamite from Bell Pit, Newry, Maine, U.S.A (Dunn – Appleman 1977)

The phase ***UNK1*** contains major Ca, Al, Si, P and usually lower contents of Sr and F (Table 3). The general formula of perhamite-like minerals is $A_3B_7(T_{(1)}O_4)_3(T_{(2)}O_4)_4X_3 \cdot 16.5H_2O$. The A-site contains M^{1+} and M^{2+} elements, in particular Ca, Sr, and Na; *B*-site contains M^{3+} and M^{4+} elements, dominant Al and minor Fe^{3+} and Ti. The first tetrahedral $T_{(1)}$-site hosts dominant Si, which can be partly substituted by Al (Mills *et al.* 2004); the $T_{(2)}$-site is occupied by P, strongly dominating over As. The *X*-site in addition to (OH) and subordinate Cl contains fluorine.

The A-site in ***UNK1*** from Krásno (Fig. 6) contains Ca (1.82–2.57 *apfu*), but in difference to perhamite from Newry Hill (Dunn – Appleman 1977), there are moderate contents of Sr (0.06 to 0.72 *apfu*) and minor contents of Zn (max. 0.10), K (0.07), Na (0.04), Ba, Mn (0.02) and Pb (max. 0.01 *apfu*). The occupancy of the *A*-site (2.51–2.84 *apfu*) indicates possible vacancies. The *B*-site

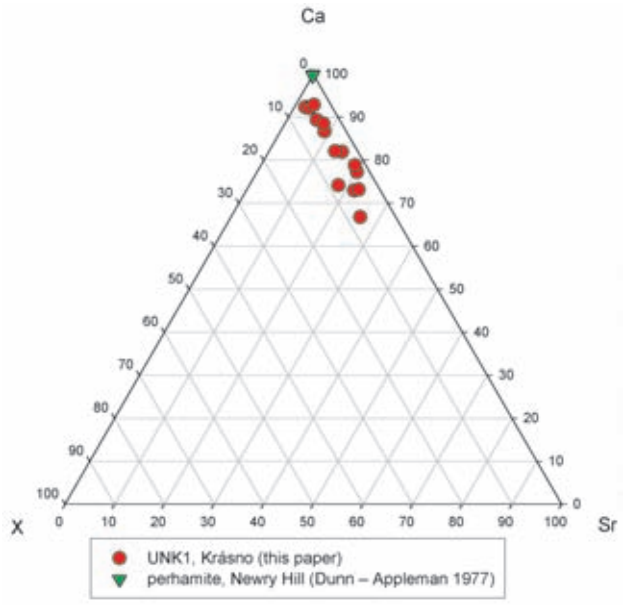

Fig. 6 Ternary plot Ca-Sr-X of occupancy of the *A*-site (atomic ratio) for ***UNK1*** from Krásno. X = Na+K+Zn+Ba+Pb+Mn.

Table 3 Chemical composition of ***UNK1*** (in wt. %)

	mean	1	2	3	4	5	6	7	8	9	10	11	12	13
Na_2O	0.06	0.04	0.06	0.09	0.04	0.09	0.04	0.08	0.11	0.04	0.01	0.00	0.07	0.08
K_2O	0.16	0.14	0.15	0.26	0.13	0.16	0.13	0.22	0.24	0.09	0.13	0.22	0.08	0.13
CaO	10.18	8.45	8.78	9.05	9.22	11.59	11.36	11.19	11.00	9.58	9.63	11.20	9.68	11.68
BaO	0.07	0.22	0.00	0.00	0.08	0.07	0.00	0.24	0.00	0.00	0.04	0.20	0.04	0.10
SrO	3.07	6.11	4.85	4.07	5.26	0.53	0.73	1.41	2.09	4.62	3.23	1.83	4.32	0.85
PbO	0.04	0.13	0.00	0.23	0.10	0.04	0.00	0.03	0.04	0.00	0.00	0.00	0.00	0.00
MnO	0.04	0.11	0.06	0.05	0.05	0.06	0.06	0.07	0.04	0.03	0.02	0.05	0.00	0.00
ZnO	0.28	0.68	0.44	0.57	0.30	0.37	0.45	0.04	0.07	0.19	0.26	0.14	0.06	0.14
Al_2O_3	30.18	30.76	32.71	28.73	30.74	29.78	30.34	29.39	29.33	30.00	30.56	29.74	29.79	30.43
Fe_2O_3	0.38	1.06	0.48	0.32	0.40	0.21	0.25	0.08	0.05	1.46	0.55	0.01	0.04	0.05
SiO_2	12.72	10.35	10.99	11.03	12.05	13.06	13.21	13.87	13.28	13.21	13.11	13.09	14.23	13.90
As_2O_5	0.05	0.17	0.00	0.03	0.00	0.08	0.00	0.00	0.06	0.14	0.09	0.00	0.03	0.00
P_2O_5	23.43	25.03	26.11	23.22	24.68	22.91	22.31	22.84	22.61	22.84	23.40	22.85	22.83	22.92
SO_3	0.02	0.00	0.06	0.08	0.05	0.00	0.00	0.00	0.02	0.00	0.03	0.00	0.02	0.00
TiO_2	0.18	0.09	0.34	0.55	0.52	0.18	0.11	0.11	0.08	0.14	0.05	0.12	0.05	0.07
Cl	0.01	0.01	0.00	0.02	0.02	0.01	0.00	0.00	0.01	0.01	0.01	0.01	0.00	0.01
F	2.88	3.34	3.10	2.78	2.96	3.21	3.06	2.54	2.70	2.08	3.19	2.75	2.93	2.76
H_2O*	23.27	23.41	23.86	23.16	23.35	23.13	23.05	23.33	23.25	23.29	23.05	23.31	22.91	23.36
O=F,Cl	-1.21	-1.40	-1.31	-1.17	-1.25	-1.35	-1.29	-1.07	-1.14	-0.88	-1.34	-1.16	-1.24	-1.16
total	105.82	108.69	110.68	103.07	108.69	104.12	103.81	104.34	103.84	106.82	106.01	104.34	105.83	105.31
Na^+	0.022	0.015	0.021	0.039	0.017	0.034	0.017	0.032	0.043	0.014	0.003	0.000	0.026	0.031
K^+	0.042	0.036	0.037	0.070	0.034	0.043	0.033	0.058	0.063	0.022	0.034	0.058	0.021	0.034
Ca^{2+}	2.232	1.846	1.827	2.094	1.990	2.566	2.503	2.471	2.459	2.080	2.081	2.490	2.113	2.531
Ba^{2+}	0.006	0.017	0.000	0.000	0.006	0.006	0.000	0.019	0.000	0.000	0.003	0.016	0.003	0.008
Sr^{2+}	0.364	0.722	0.546	0.509	0.614	0.063	0.087	0.168	0.253	0.543	0.378	0.220	0.510	0.100
Pb^{2+}	0.002	0.007	0.000	0.013	0.005	0.002	0.000	0.001	0.002	0.000	0.000	0.000	0.000	0.000
Mn^{2+}	0.008	0.019	0.009	0.010	0.008	0.010	0.011	0.012	0.006	0.004	0.004	0.009	0.000	0.000
Zn^{2+}	0.043	0.102	0.064	0.090	0.045	0.056	0.068	0.006	0.011	0.029	0.038	0.022	0.008	0.021
Al^{3+}	7.275	7.390	7.491	7.309	7.298	7.253	7.357	7.141	7.215	7.166	7.263	7.271	7.152	7.255
Fe^{3+}	0.059	0.163	0.070	0.053	0.060	0.032	0.039	0.012	0.008	0.223	0.084	0.001	0.007	0.008
Ti^{4+}	0.028	0.014	0.050	0.090	0.078	0.028	0.017	0.017	0.013	0.021	0.007	0.019	0.007	0.010
Si^{4+}	2.602	2.110	2.135	2.381	2.426	2.699	2.718	2.859	2.773	2.677	2.644	2.715	2.898	2.812
As^{5+}	0.005	0.018	0.000	0.003	0.000	0.009	0.000	0.000	0.007	0.015	0.009	0.000	0.003	0.000
P^{5+}	4.057	4.320	4.295	4.242	4.209	4.007	3.886	3.987	3.995	3.919	3.995	4.012	3.937	3.925
S^{6+}	0.003	0.000	0.009	0.013	0.007	0.000	0.000	0.000	0.003	0.000	0.005	0.000	0.003	0.000
Cl^-	0.003	0.002	0.000	0.008	0.005	0.005	0.001	0.000	0.005	0.002	0.003	0.002	0.000	0.002
F^-	1.861	2.151	1.905	1.898	1.885	2.100	1.991	1.653	1.782	1.335	2.035	1.806	1.890	1.763
H^+	33.968	35.007	34.616	34.744	34.477	33.617	33.238	33.819	33.980	33.866	33.271	34.031	33.327	33.559
OH	0.964	2.000	1.619	1.749	1.474	0.620	0.241	0.824	0.972	0.863	0.274	1.027	0.326	0.553
H_2O	16.502	16.504	16.499	16.497	16.501	16.499	16.499	16.497	16.504	16.501	16.498	16.502	16.500	16.503

mean and 1–13 spot analyses of ***UNK1***

H_2O* content was calculated from the general formula (H_2O = 16.50) and charge balance; empirical formulas were calculated on the basis of (P+As+Si+S+Al+Fe+Ti) = 14.

in ***UNK1*** is filled by dominant Al and minor Ti (max. 0.09 *apfu*) and Fe (0.22 *apfu*) (Fig. 7). With regard to the high occupancy of the *B*-site (7.17–7.61 *apfu*) it is probable that a part of Al (0.17–0.61 *apfu*) substitutes for Si in the $T_{(1)}$-site (Mills *et al.* 2004) and the *B*-site contains 6.76–6.99 *apfu* Al.

The tetrahedral $T_{(1)}$-site in ***UNK1*** is occupied by Si (2.11–2.90 *apfu*) and probably by a part of Al (0.17–0.61 *apfu*). The occupancy of the site ranges from 2.68 to 3.13 *apfu.* In the second tetrahedral $T_{(2)}$-site, phosphorus is the dominant element (3.89–4.32 *apfu*), while the contents of S and As are minor (to 0.01, 0.02 *apfu*, respectively). The total occupancy of the site is 3.89–4.34 *apfu*. Data in Fig. 8 suggest that in some analyses P may partly enter the $T_{(1)}$-site or they may indicate deviations in the ratio of $T_{(1)}$:$T_{(2)}$ from the theoretical value of 3:4 (see disorder domains in the crystal structure of perhamite, Mills *et al*. 2004).

The *X*-site in ***UNK1,*** in difference from the data for perhamite (Dunn – Appleman 1977), contains significant F corresponding to 1.34–2.15 *apfu*. Low and variable Cl is below 0.01 *apfu* and (OH) content calculated by difference corresponds to 0.24–2.00 *apfu*. The total occupancy of the *X*-site varies in dependence on charge balance for individual analyses from 2.20 to 4.15 *apfu.* All analyses of ***UNK1*** indicate that fluorine is the dominant element in the *X*-site (Fig. 9). The empirical formula for ***UNK1***, derived from the mean of 13 spot analyses on the basis of (P+As+Si+S+Al+Fe+Ti) = 14 and the above assumptions, is $(Ca_{2.23}Sr_{0.36}Zn_{0.04}K_{0.04}Na_{0.02}Ba_{0.01}Mn_{0.01})_{\Sigma 2.71}$ $(Al_{6.91}Fe_{0.06}Ti_{0.03})_{\Sigma 7.00}[(Si_{2.60}Al_{0.36})O_4]_{\Sigma 2.96}[(PO_4)_{4.06}(AsO_4)_{0.01}]_{\Sigma 4.07}$ $[F_{1.86}(OH)_{0.96}]_{\Sigma 2.83}$. $16.5H_2O$.

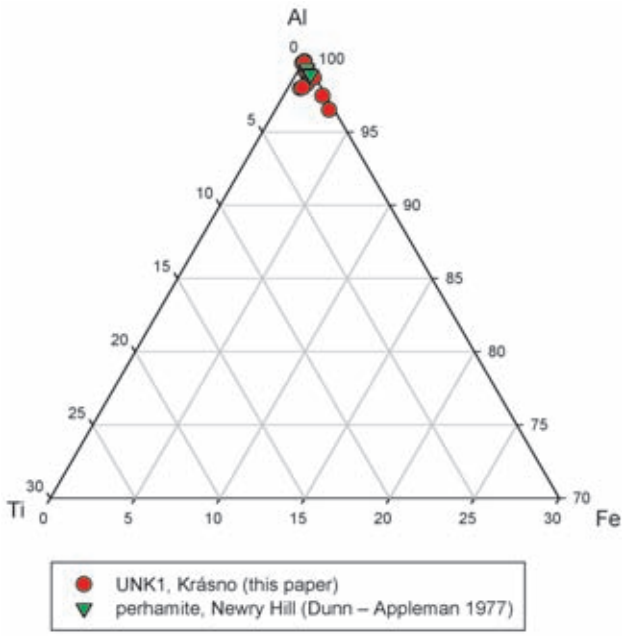

Fig. 7 Part of ternary plot Al (in *B*-site)-Ti-Fe of the *B*-site occupancy (atomic ratios) for ***UNK1*** from Krásno.

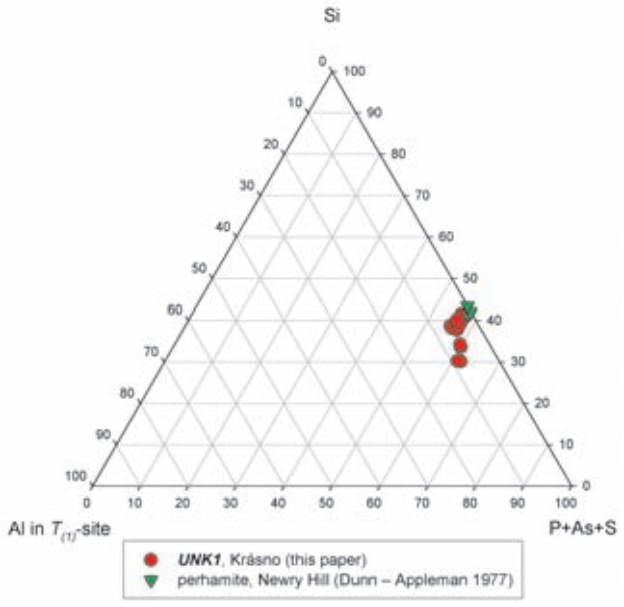

Fig. 8 Ternary plot Si-Al in $T_{(1)}$-site-(P+As+S) of *T*-sites occupancy (atomic ratios) for ***UNK1*** from Krásno.

UNK2 Cu arsenate – $Cu_{13}(AsO_4)_6(AsO_3OH)_4 \cdot 23H_2O$ (IMA 2004-38)

The phase ***UNK2*** has been found in the Huber open pit. It occurred in proximity of a narrow and weathered ore vein, carrying tennantite and cuprite in its centre. The phase ***UNK2*** forms light blue to light blue-green crystalline coatings up to 2 by 2 cm in size, which are composed of minute and imperfect thin tabular crystals (Fig. 10). It also occurs in a mixture with clay minerals

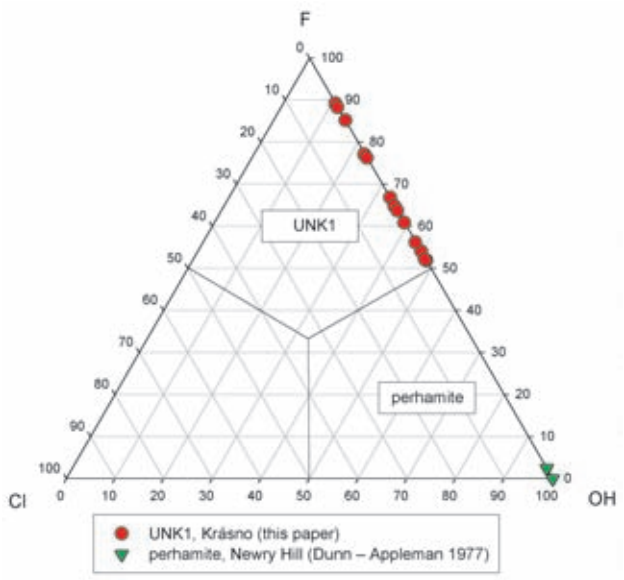

Fig. 9 Ternary plot F-Cl-(OH) of *X*-sites occupancy (atomic ratios) for ***UNK1*** from Krásno.

as light blue aggregates cementing weathered gangue, or as botryoidal aggregates in weathered greisen around the ore vein, reminiscent of chalcanthite efflorescence. X-ray amorphous arsenates of Cu and Fe in green glassy aggregates cementing gangue are closely associated with ***UNK2***.

The X-ray powder diffraction data (Table 4) and refined unit-cell parameters for ***UNK2*** from Krásno (Table 5) correspond to a recently studied new mineral from the Geschieber vein in the Jáchymov ore district (Krušné hory, Czech Republic). The samples from Jáchymov contain well-formed crystals. Results of a detailed study of this material, including determination of crystal structure based on single-crystal X-ray diffraction and quantitative chemical analysis, were submitted to the Com-

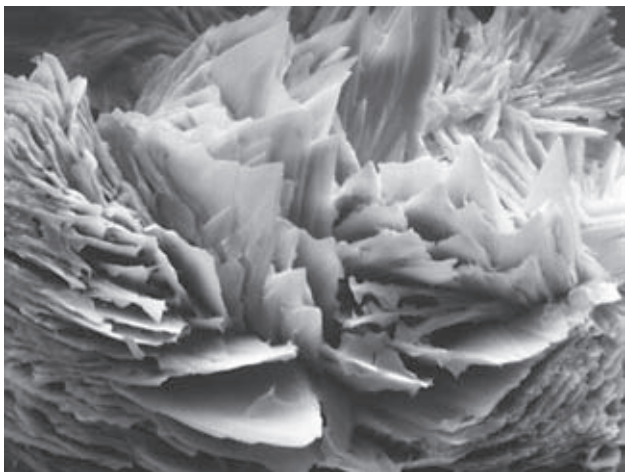

Fig. 10 Group of thin tabular crystals of ***UNK2***, Krásno. Width of the area shown 80 μm. SEM photograph Tesla BS 340, A. Gabašová.

Table 4 X-ray powder diffraction pattern of ***UNK2***

I_{rel}	d	h	k	l	I_{rel}	d	h	k	l	I_{rel}	d	h	k	l
2.7	15.775	0	0	1	0.2	3.120	1	3	1	0.4	2.2701	0	2	6
2.1	13.778	0	1	0	1.1	3.097	0	2	4	0.2	2.2660	0	-3	7
100.0	12.015	0	-1	1	0.6	3.089	0	3	3	0.2	2.2399	2	3	1
0.6	9.266	0	1	1	0.5	3.048	2	-2	0	0.5	2.2229	-1	6	1
1.8	7.006	0	-2	1	0.3	2.996	-2	-1	1	0.2	2.1996	1	4	3
3.4	6.889	0	2	0	0.3	2.992	2	-1	1	0.2	2.1687	-2	5	2
1.8	6.195	0	1	2	1.2	2.989	-2	-1	2	0.3	2.1580	1	-6	4
0.5	6.183	1	0	0	0.9	2.982	0	-3	5	0.2	2.1561	0	-4	7
0.2	6.095	1	-1	0	0.7	2.962	1	-4	3	0.2	2.1403	-2	4	4
3.0	6.008	0	-2	2	0.5	2.958	1	-3	4	0.3	2.1384	0	1	7
3.6	5.792	0	2	1	0.9	2.935	2	-2	1	0.2	2.1019	-2	-3	6
0.4	5.504	-1	-1	1	0.9	2.917	0	1	5	0.2	2.0998	-1	-5	6
0.3	5.365	1	0	1	0.4	2.905	-1	-4	1	0.2	2.0976	-1	-4	7
0.3	5.276	1	1	0	1.2	2.896	0	4	2	0.2	2.0961	2	3	2
0.4	5.258	0	0	3	0.2	2.880	-2	-1	3	0.2	2.0919	-1	5	4
0.3	5.121	-1	-1	2	1.9	2.841	0	-5	1	0.2	2.0671	0	6	2
0.7	5.093	-1	1	2	0.5	2.838	0	-5	2	0.2	2.0357	1	-6	5
0.3	4.858	-1	2	1	0.3	2.812	1	3	2	0.3	2.0292	1	6	0
1.0	4.748	0	-3	1	0.2	2.795	1	1	4	0.4	2.0278	0	5	4
1.4	4.633	0	2	2	0.2	2.762	2	-3	1	0.3	2.0213	0	-7	3
0.2	4.618	1	1	1	0.5	2.752	-2	-2	2	0.4	2.0206	1	-7	2
0.2	4.592	1	-1	2	0.7	2.751	1	-5	1	0.3	2.0162	0	-5	7
0.4	4.540	0	1	3	0.7	2.748	0	-5	3	0.2	2.0098	2	4	1
0.3	4.281	-1	2	2	0.2	2.746	2	-2	2	0.2	2.0047	1	4	4
0.2	4.217	1	2	0	0.7	2.702	-2	3	2	0.2	2.0015	-1	-6	5
0.3	4.134	0	3	1	0.2	2.702	1	-5	2	0.3	1.9960	0	2	7
0.4	4.030	1	-3	1	0.2	2.698	0	-2	6	0.2	1.9959	-1	-3	8
0.3	3.937	-1	-2	3	0.6	2.689	-2	-2	3	0.2	1.9854	-1	6	3
0.3	3.876	-1	3	1	0.4	2.629	0	0	6	0.2	1.9719	0	0	8
0.4	3.792	1	2	1	0.3	2.624	2	-3	2	0.2	1.9682	0	7	0
0.2	3.723	-1	0	4	0.2	2.612	-1	5	1	0.3	1.9561	2	-6	3
0.2	3.626	1	0	3	0.8	2.604	0	5	1	0.3	1.9384	-2	5	4
0.7	3.589	0	3	2	0.5	2.560	-2	-2	4	0.3	1.9380	-1	4	6
0.5	3.548	-1	-3	1	0.4	2.546	-2	2	4	0.2	1.9271	1	-7	4
1.0	3.539	-1	-3	2	0.5	2.540	-2	3	3	0.2	1.9120	-2	2	7
0.2	3.463	0	-3	4	0.2	2.514	1	3	3	0.2	1.9107	3	-4	1
3.4	3.444	0	4	0	0.2	2.505	-2	0	5	0.6	1.9066	-1	-6	6
0.5	3.389	1	3	0	0.3	2.4875	2	2	1	0.2	1.8852	2	5	0
0.3	3.365	-1	-3	3	0.2	2.4556	-1	5	2	0.4	1.8611	-1	-7	3
0.2	3.358	1	-3	3	0.2	2.4395	-1	-5	1	0.3	1.8533	0	5	5
2.3	3.294	0	-4	3	0.3	2.4380	2	0	3	0.2	1.8371	2	-7	1
0.9	3.281	1	1	3	0.7	2.4202	1	-5	4	0.3	1.8295	-1	-7	1
0.8	3.263	0	-1	5	1.1	2.4090	0	-4	6	0.2	1.8268	2	-7	0
1.0	3.199	0	4	1	0.3	2.4031	0	-5	5	0.2	1.7944	0	6	4
0.2	3.195	0	-2	5	0.8	2.3742	0	-6	2	0.4	1.7794	1	7	0
0.2	3.170	-2	0	1	0.2	2.3624	-1	-5	4	0.2	1.7764	2	4	3
0.3	3.161	1	-1	4	0.2	2.3545	1	5	0	0.2	1.7739	-2	-6	2
0.7	3.155	0	0	5	0.4	2.3359	0	3	5	0.2	1.7433	-2	-6	1
0.4	3.149	2	-1	0	0.2	2.3207	1	-6	2	0.3	1.7126	1	7	1
0.2	3.142	-1	4	1	0.5	2.3092	2	2	2	0.3	1.7062	-3	-4	2

Table 5 Unit-cell parameters of ***UNK2*** (for triclinic space group *P*-1)

	Krásno this paper	Jáchymov IMA 2004-038
a [Å]	6.407(7)	6.408(3)
b [Å]	14.402(7)	14.491(5)
c [Å]	16.60(2)	16.505(8)
α [°]	102.89(6)	102.87(3)
ß [°]	100.5(1)	101.32(5)
γ [°]	98.23(8)	97.13(3)
V [Å^3]	1441	1442(1)

mission on New Minerals and Mineral Names of the International Mineralogical Association. The proposal was approved by the Commission as a new mineral under the number IMA 2004-38.

The chemical composition of ***UNK2*** from Krásno has been studied with EMPA (energy-dispersion type) only in a semi-quantitative way. Cu and As are the major elements. This is in good agreement with the quantitative chemical data for the proposed mineral from Jáchymov,

which yielded the ideal formula $Cu_{13}(AsO_4)_6(AsO_3OH)_4 \cdot 23\ H_2O$.

UNK3 Zn-Fe phosphate (rockbridgeite-like) – $Zn(Fe,Zn,Al)_4(PO_4)_3(OH)_4$

The mineral phase ***UNK3*** has been noted in several samples of phosphate accumulations in the Huber open pit (Sejkora *et al.* 2006c). Since morphology of ***UNK3*** and its hosting asseblages vary significantly, individual types of occurrence are described separately.

The first type of ***UNK3*** occurs in a 6 cm long fragment of triplite aggregate, altered to compact red-brown fluorapatite and isokite. This material is accompanied by coarse-grained white quartz containing up to 2 cm long grains of dark green fluorapatite. Cavities in this material, 1–2 cm in diameter, carry semi-spherical to spheroidal, radiating aggregates of ***UNK3*** up to 1.5 mm in size (Fig. 11), locally grouped to aggregates 5 mm long (Fig. 12). The cavities also carry imperfect crystals of light yellow-grey younger fluorapatite. The aggregates of ***UNK3*** (Fig. 13) are black-green to black with a green

Fig. 11 Black-green spheroidal aggregates of ***UNK3*** with light fluorapatite. Huber open pit, Krásno. Width of the area shown 2.1 mm. Nikon SMZ1500, photograph by J. Sejkora.

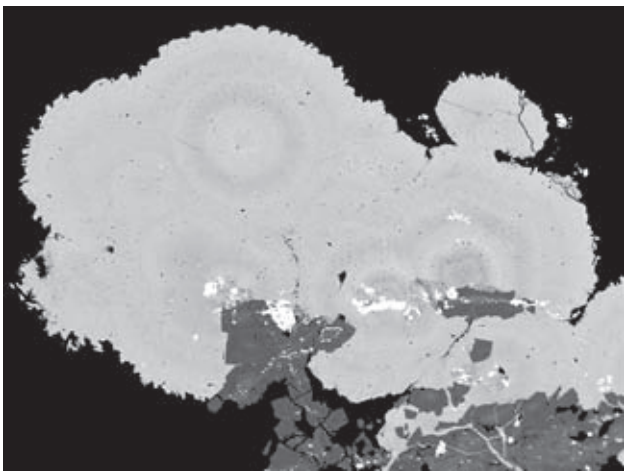

Fig. 12 Semi-spheroidal aggregates of ***UNK3***, showing a weak zoning, with inclusions of Fe oxides-hydroxides (white) deposited on fluorapatite (dark grey), with minute inclusions of Nb-rutile (light). Width of the area shown 2 mm. Cameca SX100 BSE photograph by J. Sejkora and R. Škoda.

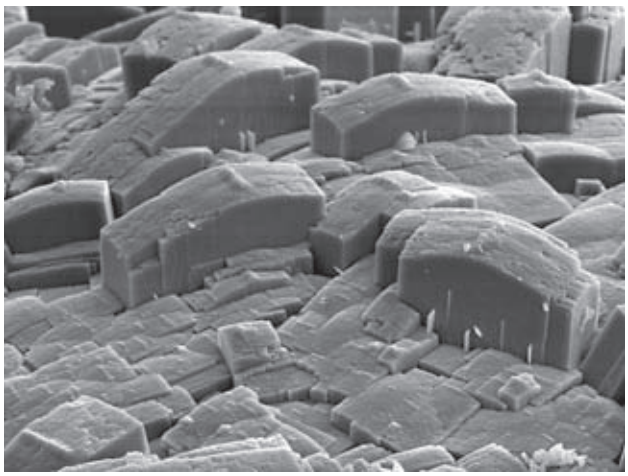

Fig. 13 Detail of surface of spherical aggregates of ***UNK3*** (the first type), Krásno. Width of the area shown 75 μm. SEM photograph Jeol JSM-6380, J. Sejkora and J. Plášil.

shade, vitreous on fracture, with a greasy lustre. Minute splinters are transparent, bright green, and have a light grey-green streak.

The second type of ***UNK3*** has been found in strongly altered aggregate of pinkish and white fluorapatite, 7 by 10 cm in size. The phase forms soft and crumbly grey-green aggregates up to 2 cm long in irregular cavities 5 by 6 cm in size. The aggregates consist of minute crystals (to 0.1 mm), intergrown with frequent light green fluorapatite and less abundant kolbeckite aggregates. Well-formed tabular crystals of ***UNK3*** (Fig. 14) are black with a green shade, and vitreous lustre.

The third type of ***UNK3*** has been found in weathered vugs, 2 by 3 cm in size, in fluorapatite/isokite accumulations with triplite relics. The phase forms dark green crystalline aggregates with a strong vitreous lustre, 0.5–1 mm in size. The aggregates (Fig. 15) are composed of tabular crystals to 0.1 mm long, showing occasional rhombic cross-sections. Such aggregates (Fig. 16) are usually overgrown by zoned aggregates of the turquoise-group minerals, including UNK10, pharmacosiderite, UNK1, rare kolbeckite and Cl-rich fluorapatite. ***UNK3*** of microscopic size occurs in additional two associations of phosphate accumulations: irregular inclusions to

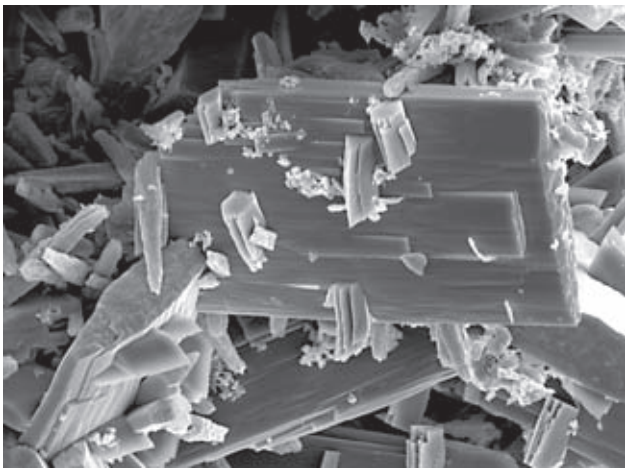

Fig. 14 Tabular crystals of ***UNK3*** (the second type), Krásno. Width of the area shown 80 μm. SEM photograph Jeol JSM-6380, J. Sejkora and J. Plášil.

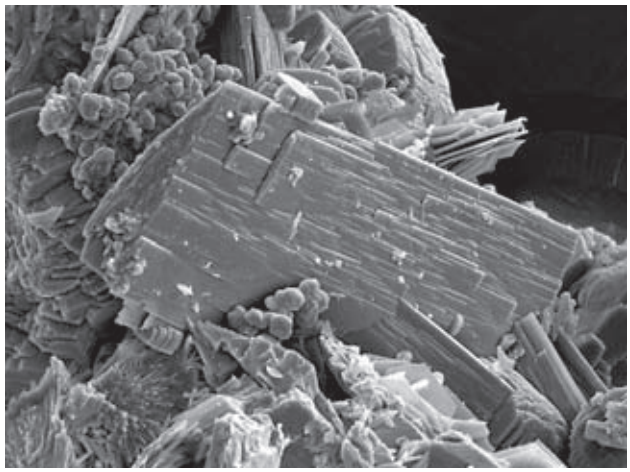

Fig. 15 Tabular crystals of the third type of ***UNK3***, Krásno. Width of the area shown 110 μm. SEM photograph Jeol JSM-6380, J. Sejkora and J. Plášil

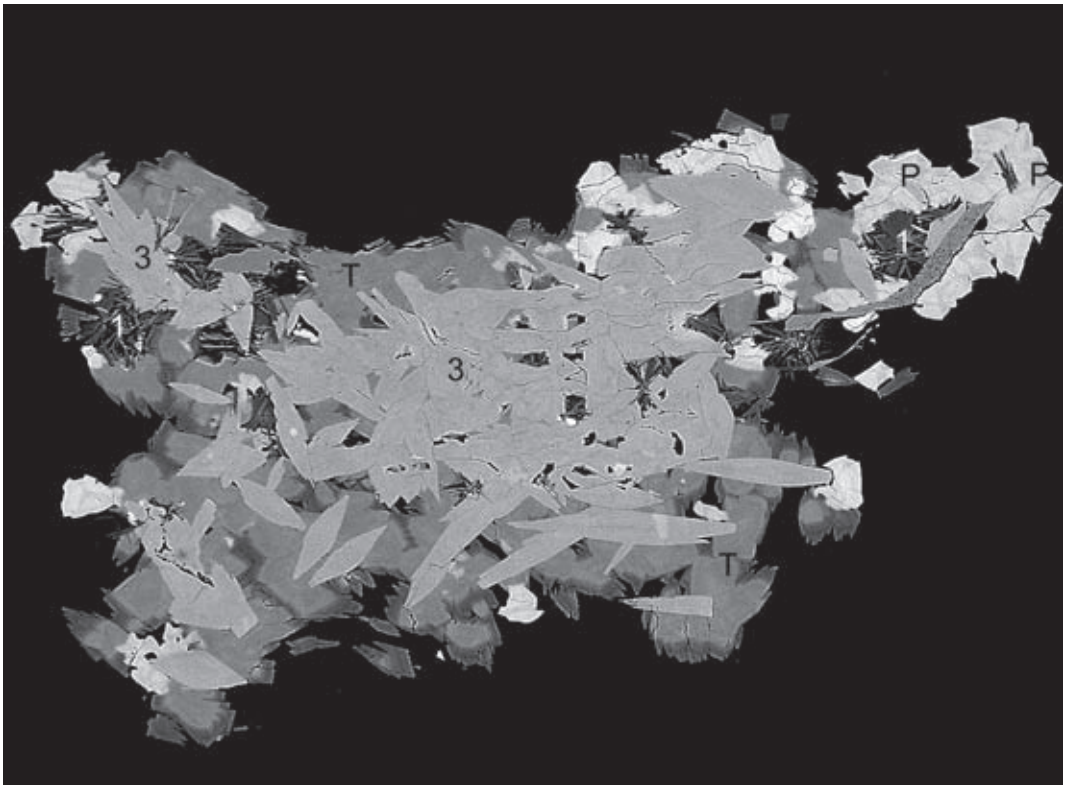

Fig. 16 Aggregate of tabular crystals of ***UNK3*** (in places with rhombic sections – 3), overgrown by zoned aggregate of turquoise group minerals (T) and ***UNK1*** (prominently tabular – 1). Pharmacosiderite crystals (light – P) are present at the margin of the aggregate. Width of the area shown 500 μm. Cameca SX100, BSE photograph by J. Sejkora and R. Škoda.

Table 6 X-ray powder diffraction pattern of ***UNK3***

I_{rel}	*d*	*h*	*k*	*l*	I_{rel}	*d*	*h*	*k*	*l*	I_{rel}	*d*	*h*	*k*	*l*
4	8.390	0	0	2	11	2.5790	2	0	0	8	1.8293	2	2	6
68	6.916	0	2	0	20	2.4209	1	1	6	10	1.7950	0	4	8
10	4.824	1	1	0	17	2.4128	1	5	1	14	1.7307	0	8	0
3	4.648	1	1	1	14	2.4011	1	3	5	12	1.7107	1	5	7
18	4.352	0	2	3	4	2.3448	1	5	2	6	1.6961	0	8	2
40	4.195	0	0	4	21	2.2667	0	2	7	9	1.6853	2	6	2
17	3.656	1	1	3	7	2.2242	0	6	2	16	1.6798	0	0	10
46	3.590	0	2	4	3	2.1687	1	3	6	17	1.6420	0	4	9
19	3.438	1	3	0	8	2.1476	1	1	7	11	1.6007	0	8	4
100	3.390	0	4	1	7	2.1080	1	5	4	13	1.5903	2	6	4
48	3.182	1	3	2	3	2.0977	2	2	4	13	1.5526	0	6	8
25	3.021	0	2	5	7	2.0547	2	4	1	6	1.5312	2	6	5
6	2.945	0	4	3	17	2.0221	0	6	4	12	1.4659	2	6	6
18	2.799	0	0	6	11	1.9606	2	2	5	7	1.4583	3	1	6
20	2.755	1	1	5	9	1.8989	2	0	6					
11	2.672	0	4	4	11	1.8465	1	7	0					

30 μm in beraunite associated with K-poor leucophosphite and irregular aggregates (max. 100 μm) with fluorapatite, isokite, whitmoreite and UNK1.

The X-ray powder diffraction data for the first and second morphological types of ***UNK3*** are practically identical. Detailed work has been done on sample of the first type (Table 6). Since the data are similar to published values for minerals of the series rockbridgeite – frondelite, indexing was done using a model derived from the crystal structure data for rockbridgeite (Moore 1970) (full occupancy of *M(a)*-site Zn, *M(b)*-sites Fe^{3+}). The refined unit-cell parameters for UNK3 (Table 7) are very close to data for rockbridgeite.

The quantitative chemical composition of several morphologically distinct ***UNK3*** types was obtained on five individual samples. The average of all 19 analyses and eight representative analyses are given in Table 8. The chemical composition for the morphological types described above is very similar. Since X-ray diffraction data for individual morphological types of ***UNK3*** and minerals of the rockbridgeite-frondelite series are similar, the chemical analyses were re-calculated on the basis of (P+As+Si+S) = 3 of the general formula $M(a)M(b)_4(PO_4)_3(OH)_5$. Lower totals of the analyses in the range of 94–97 wt. %, after inclusion of the theoretical content of H_2O (corresponding to OH groups), indicate a possible presence of about 2 water molecules in the phase ***UNK3***.

The chemical composition of ***UNK3*** from Krásno (Table 8) is greatly variable and more importantly, represents the highest Zn content, known at present in minerals related to rockbridgeite – frondelite. In the following text we assume that the M^{1+} a M^{2+} cations preferentially occupy *M(a)* site and Zn^{2+} surplus (above the total of *M(a)* site = 1) enters the *M(b)* sites, together with Fe^{3+}, Al^{3+} and Ti^{4+}. In addition to minor and irregular contents of Ba and Pb (max. 0.01 *apfu*) in the *M(a)* site, there are somewhat higher contents of Ca (0.02–0.07 *apfu*), Mn (0–0.10 *apfu*), Na (0.01–0.12 *apfu*) and dominant Zn in the range of 0.73 to 0.90 *apfu* (Fig. 17). The *M(b)* sites (Fig. 18) contain minor and irregular Ti (max. 0.06 *apfu*),

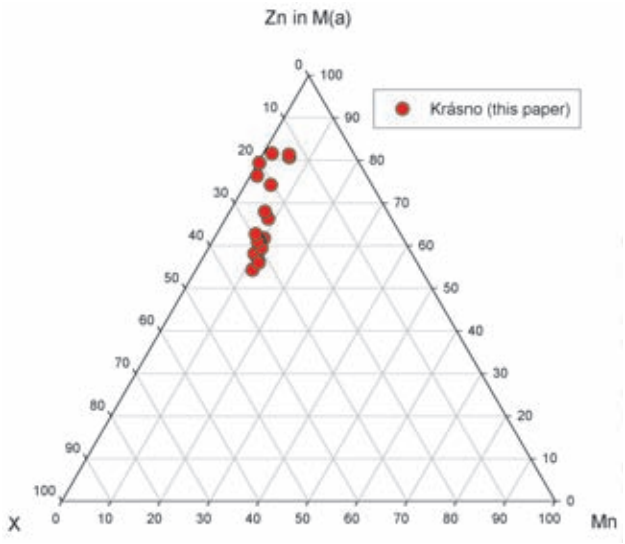

Fig. 17 Ternary plot of Mn-(Zn in M(a))-X of *M(a)*-site occupancy (atomic ratios) for ***UNK3*** from Krásno. X = Na, Ca, Ba and Pb in *M(a)*-site.

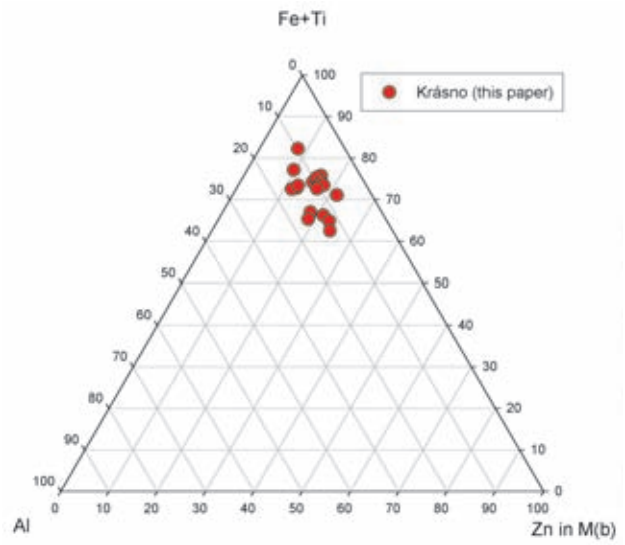

Fig. 18 Ternary plot of (Zn in M(b))–(Fe+Ti)-Al of *M(b)*-site occupancy (atomic ratios) for ***UNK3*** from Krásno.

Table 7 Unit-cell parameters of ***UNK3*** (for orthorhombic space group *Cmcm*)

	UNK3 this paper	rockbridgeite 1*	frondelite 2*
a [Å]	5.161(1)	5.172–5.185	5.176–5.210
b [Å]	13.846(2)	13.78–13.873	13.810–13.932
c [Å]	16.789(3)	16.782–16.810	16.811–17.010
V [Å^3]	1199.8(3)	1198.0–1207.1	1211.4–1231.0

*1 various occurrences, Sejkora *et al.* (2006c), Moore (1970), ICDD 34-150.
*2 various occurrences, Sejkora *et al.* (2006c), ICDD 8-83, 35-625.

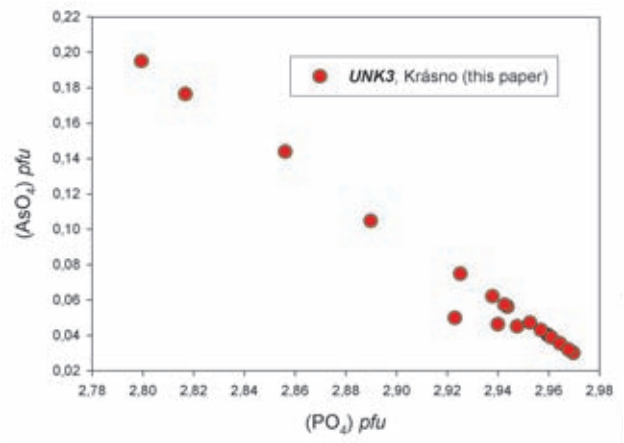

Fig. 19 Plot of (PO_4) – (AsO_4) *pfu* in tetrahedral site of ***UNK3*** from Krásno.

Table 8 Chemical composition of ***UNK3*** (wt. %)

	mean	1	2	3	4	5	6	7	8
Na_2O	0.42	0.41	0.37	0.34	0.44	0.50	0.04	0.56	0.46
K_2O	0.02	0.03	0.00	0.04	0.00	0.03	0.01	0.01	0.04
CaO	0.43	0.32	0.29	0.14	0.56	0.49	0.36	0.41	0.52
BaO	0.06	0.00	0.00	0.18	0.04	0.12	0.14	0.00	0.16
SrO	0.02	0.05	0.00	0.04	0.00	0.01	0.03	0.03	0.06
MgO	0.02	0.00	0.03	0.01	0.02	0.03	0.02	0.01	0.02
PbO	0.04	0.09	0.10	0.00	0.00	0.01	0.00	0.00	0.10
CuO	0.01	0.00	0.00	0.06	0.00	0.00	0.00	0.00	0.00
MnO	0.72	0.77	0.45	0.14	1.01	0.86	0.47	1.11	0.73
ZnO	15.24	10.77	12.13	13.50	15.63	17.43	17.57	18.10	19.19
Al_2O_3	3.71	3.07	4.13	5.05	2.88	4.01	5.08	3.93	4.17
Fe_2O_3	36.21	39.84	37.68	35.99	37.62	32.63	32.09	32.86	30.77
SiO_2	0.05	0.01	0.05	0.05	0.02	0.03	0.00	0.01	0.04
TiO_2	0.20	0.70	0.34	0.10	0.01	0.68	0.22	0.52	0.74
As_2O_5	1.22	1.31	1.82	3.36	0.72	1.14	0.77	1.01	0.86
P_2O_5	32.15	31.58	30.97	29.76	32.96	33.19	32.75	31.93	33.26
SO_3	0.03	0.05	0.20	0.03	0.00	0.00	0.07	0.00	0.00
Cl	0.01	0.00	0.00	0.00	0.00	0.01	0.01	0.01	0.01
H_2O*	5.59	5.90	5.81	5.95	5.57	4.97	5.15	5.63	4.85
total	96.14	94.88	94.36	94.72	97.48	96.13	94.78	96.12	96.00
Na^+	0.088	0.086	0.078	0.074	0.091	0.101	0.009	0.118	0.094
K^+	0.002	0.005	0.000	0.006	0.000	0.004	0.001	0.002	0.006
Ca^{2+}	0.049	0.037	0.035	0.016	0.064	0.055	0.041	0.048	0.059
Ba^{2+}	0.002	0.000	0.000	0.008	0.002	0.005	0.006	0.000	0.007
Sr^{2+}	0.001	0.003	0.000	0.002	0.000	0.001	0.002	0.002	0.004
Mg^{2+}	0.003	0.000	0.005	0.001	0.003	0.004	0.003	0.002	0.003
Pb^{2+}	0.001	0.003	0.003	0.000	0.000	0.000	0.000	0.000	0.003
Cu^{2+}	0.001	0.000	0.000	0.005	0.000	0.000	0.000	0.000	0.000
Mn^{2+}	0.065	0.072	0.042	0.014	0.091	0.076	0.043	0.102	0.065
Zn^{2+}	1.209	0.869	0.982	1.107	1.223	1.344	1.381	1.455	1.484
Al^{3+}	0.470	0.396	0.533	0.661	0.359	0.493	0.637	0.504	0.515
Fe^{3+}	2.927	3.275	3.108	3.007	3.001	2.565	2.570	2.690	2.425
Ti^{4+}	0.016	0.057	0.028	0.008	0.001	0.053	0.017	0.042	0.058
Si^{4+}	0.005	0.001	0.005	0.006	0.002	0.003	0.000	0.001	0.004
As^{5+}	0.069	0.075	0.104	0.195	0.040	0.062	0.043	0.057	0.047
P^{5+}	2.924	2.920	2.874	2.797	2.958	2.935	2.952	2.942	2.949
S^{6+}	0.002	0.004	0.016	0.002	0.000	0.000	0.005	0.000	0.000
Cl^-	0.001	0.000	0.000	0.000	0.000	0.002	0.001	0.001	0.002
OH	4.006	4.299	4.249	4.407	3.939	3.463	3.657	4.086	3.388
Zn in *M(a)*	0.787	0.795	0.838	0.873	0.749	0.754	0.895	0.727	0.761
total *M(a)*	1.000	1.000	1.000	1.000	1.000	1.000	1.000	1.000	1.000
Zn in *M(b)*	0.422	0.074	0.144	0.233	0.474	0.591	0.486	0.728	0.723
total *M(b)*	3.836	3.802	3.813	3.910	3.835	3.703	3.711	3.965	3.721

mean of all 19 spot analyses, 1–8 – representative spot analyses.
Empirical formulas were calculated on the basis of (P+As+Si+S) = 3;
H_2O* content was calculated from the charge balance of general formula.

Al in the range of 0.30 to 0.66 *apfu* and Zn 0.07–0.72 *apfu*. The Fe^{3+} contents are c. 2.43 to 3.28 *apfu*; the total occupancy of the *M(b)* site, 3.61–3.96 *apfu* is near the theoretical content of 4 *apfu.*

The anion group in ***UNK3*** contains dominant P (2.80–2.97 *apfu*), invariably As (0.03–0.19 apfu), and variably minor Si (max. 0.02 *apfu*) (Fig. 19). The presence of M^{1+} elements in *M(a)*-site and a significant content of Zn in *M(b)*-sites result in decrease of (OH) groups from five (frondelite, rockbridgeite) to four in ***UNK3*** (the calculated range of 3.40–4.40 (OH) *pfu*). The empirical formula for ***UNK3*** $(Zn_{0.79}Na_{0.09}Mn_{0.07}Ca_{0.05})_{\Sigma 1.00}(Fe_{2.93}Zn_{0.42}Al_{0.47}Ti_{0.02})_{\Sigma 3.84}[(PO_4)_{2.92}(AsO_4)_{0.07}]_{\Sigma 2.99}(OH)_{4.01}$ can be simplified to an ideal formula $Zn(Fe,Zn,Al)_4(PO_4)_3(OH)_4$.

UNK4 CaAl phosphate fluoride – trigonal (?)

$CaAl_3(PO_4)(PO_3OH)(OH,F)_6$ (?)

UNK4 has been found in one phosphate accumulation sample collected at the 5th level of the Huber shaft, Krásno (Sejkora *et al.* 2006c). The sample is composed dominantly of compact brownish fluorapatite free of obvious triplite relics and some massive white quartz. The phase ***UNK4*** occurs as crystalline coatings 2.5 by 3 cm in size (Fig. 20) in irregular cavity of brownish fluorapatite. The associated minerals include abundant white to light pink younger fluorapatite and local green aggregates of minerals of the chalcosiderite-turquoise series. The surface of the ***UNK4*** coatings is

formed by 0.3 mm long aggregates of minute and very thin tabular crystals with maximum size of 0.1–0.2 mm (Fig. 21). The very brittle and soft ***UNK4*** aggregates are white, yellowish or light pink. The aggregates have pearly lustre, individual transparent to translucent crystals have a vitreous lustre.

The sample studied by X-ray powder diffraction contained in addition to dominating phase ***UNK4*** a significant admixture of fluorapatite (Table 9), which prevented reliable indexing of the diffractions. The X-ray data for ***UNK4*** were indexed based on similarity with crandallite in the space group *P*3. The refined unit-cell parameters are a = 6.984(1), c = 16.796(3) Å and V = 709.5(3). However, it must be noted that in the angular range correponding to d-spacing between 20 to 6 Å, the major differences between the pattern for ***UNK4*** and

Fig. 20 Whitish aggregates of ***UNK4*** from phosphate accumulation from the 5th level of the Huber shaft, Krásno. Width of the area shown 8 mm. Nikon SMZ1500, photograph by J. Sejkora.

Table 9 X-ray powder diffraction pattern of ***UNK4*** from Krásno.

I_{rel}	d		h	k	l	I_{rel}	d		h	k	l	I_{rel}	d		h	k	l
100	16.812	*	0	0	1	21	2.965	*	1	1	3	9	1.9341	F			
21	8.399	*	0	0	2	17	2.939	*	0	1	5	9	1.8971	*	0	3	3
3	8.114	F				5	2.847	*	0	2	2	4	1.8827	F			
10	6.056	*	1	0	0	37	2.799	*F	0	0	6	21	1.8670	*	0	0	9
18	5.697	*	0	1	1	10	2.772	F				9	1.8366	F			
15	5.596	*	0	0	3	29	2.702	F				6	1.8181	*	0	3	4
3	4.911	*	0	1	2	4	2.660	*	0	2	3	7	1.8120				
6	4.842					8	2.624	F				5	1.7967	*	1	1	8
7	4.202	*	0	0	4	12	2.610					4	1.7935	F			
2	4.108	*	0	1	3	10	2.543	*	0	1	6	10	1.7692	*F	2	1	6
8	4.053	F				3	2.514	F				11	1.7462	*F	2	2	0
6	3.871	F				14	2.4033	*	0	0	7	7	1.7229	*F	2	0	8
12	3.494	*	1	1	0	8	2.2893	*F	2	1	0	3	1.7097	*	2	2	2
13	3.443	*F	1	0	4	21	2.2487	*	0	2	5	7	1.6357	*F	0	3	6
15	3.341					24	2.2317	*	0	1	7	7	1.5145		1	1	10
8	3.307					2	2.1800	*	1	1	6	10	1.4683	*F	0	2	10
8	3.197					6	2.1358	F				6	1.4222		0	4	4
5	3.168	F				1	2.0606	F				5	1.3978		1	1	11
12	3.065	F				17	1.9845	*	0	1	8	7	1.3644		1	0	12

* – diffraction maxima used for refinement of unit-cell parameters in proposed primitive trigonal cell
F – probable coincidence with fluorapatite

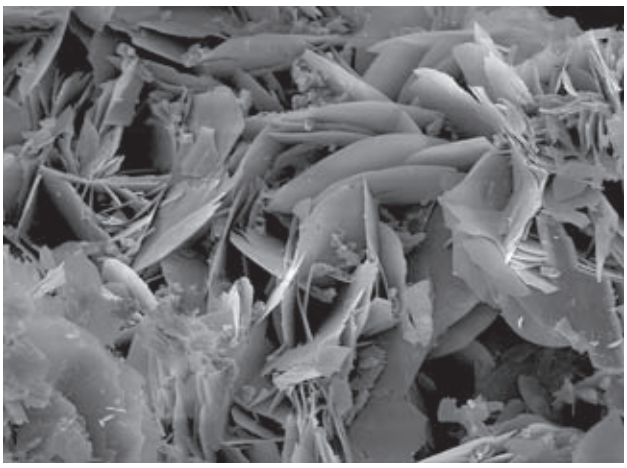

Fig. 21 Thin tabular crystals of ***UNK4***, Krásno. Width of the area shown 140 μm. SEM photograph Jeol JSM-6380, J. Sejkora and J. Plášil

those of trigonal crandallite (*R*-3*m*; Blount 1974) and probably triclinic crandallite (Cowgill *et al.* 1963) may be observed.

The quantitative chemical analyses of ***UNK4*** show major contents of Ca, Al, P a F (Table 10). Therefore, it is possible that it is a fluorine-rich mineral, structurally related to crandallite $CaAl_3(PO_4)(PO_3OH)(OH,F)_6$. The relatively low and variable analytic totals of ***UNK4*** (after including calculated H_2O content) are probably due to the surface properties of the analyzed sample, composed of very thin, tabular crystals. The chemical composition of the crandallite group minerals can be expressed by the general formula $AB_3(TO_4)(TO_3OH)(OH,F)_6$.

The *A*-site of ***UNK4*** contains dominant Ca (1.06–1.30 *apfu*) and minor K (max. 0.08), Sr (max. 0.06) and Cu (max. 0.01 *apfu*); the total for *A*-site is 1.21–1.46 *apfu*. In *B*-site Al (3.05–3.32 *apfu*) is the dominant element, Fe^{3+} content is in the range of 0.01–0.02 *apfu*; the total for *B*-site is 3.07–3.32 *apfu*. The tetrahedral *T*-site is dominated by P (1.83–1.99 *apfu*), with a local content of Si (max. 0.17 *apfu*). The relative deficiency in the *T*-site (as compared to cations in *A*- and *B*-sites) is probably compensated by increased number of (OH,F) groups of 6.42–7.72 *pfu,* compared to the theoretical number of 6.00. There is an increased content of F (2.41–2.63 *apfu*) in the (OH,F)-sites. Accepting the crandallite-type chemistry and the relation (P+As+Si+S) = 2.00, the empirical formula for ***UNK4*** is $(Ca_{1.16}K_{0.06}Ba_{0.01}Sr_{0.05})_{\Sigma 1.28}(Al_{3.24}Fe_{0.02})_{\Sigma 3.26}[(PO_3OH)_{1.00}(PO_4)_{0.91}(SiO_4)_{0.08}]_{\Sigma 1.99}[(OH)_{4.75}F_{2.51}]_{\Sigma 7.26}$.

Re-calculation of the analyses on an alternative basis is possible, e.g., assuming (P+As+Si+S) = 3. This results in the empirical formula $(Ca\ldots)_{1.97}(Al\ldots)_{4.88}[(PO_4)\ldots]_3[(OH)_{5.61}F_{3.77}]_{\Sigma 9.38}$.

Table 10 Chemical composition of ***UNK4*** from Krásno (in wt. %)

	mean	1	2	3	4
Na_2O	0.02	0.03	0.00	0.00	0.05
K_2O	0.57	0.51	0.57	0.56	0.66
CaO	12.41	12.13	11.70	13.13	12.67
MgO	0.04	0.00	0.05	0.06	0.04
PbO	0.09	0.00	0.12	0.11	0.14
CuO	0.11	0.21	0.21	0.00	0.00
ZnO	0.02	0.04	0.00	0.03	0.00
MnO	0.04	0.00	0.02	0.09	0.03
BaO	0.34	0.57	0.00	0.64	0.16
SrO	1.08	1.25	0.95	1.04	1.08
Fe_2O_3	0.30	0.35	0.39	0.23	0.23
Al_2O_3	31.35	31.77	31.22	33.13	29.30
TiO_2	0.02	0.00	0.03	0.00	0.06
SiO_2	0.93	2.11	0.00	0.77	0.83
P_2O_5	25.81	26.47	26.11	26.95	23.70
As_2O_5	0.06	0.00	0.16	0.00	0.08
SO_3	0.05	0.00	0.09	0.10	0.00
F	9.07	9.38	9.09	9.82	7.98
-O=F	-3.82	-3.95	-3.83	-4.14	-3.36
H_2O*	11.00	10.10	11.18	11.14	11.62
total	89.48	90.98	88.04	93.68	85.26
Na	0.003	0.005	0.000	0.000	0.009
K	0.064	0.053	0.065	0.061	0.080
Ca	1.164	1.060	1.126	1.189	1.297
Ba	0.012	0.018	0.000	0.021	0.006
Sr	0.055	0.059	0.049	0.051	0.060
Mg	0.005	0.000	0.006	0.007	0.006
Pb	0.002	0.000	0.003	0.003	0.004
Cu	0.007	0.013	0.014	0.000	0.000
Mn	0.003	0.000	0.002	0.007	0.002
Zn	0.001	0.002	0.000	0.002	0.000
total *A*-site	1.316	1.211	1.266	1.340	1.464
Al^{3+}	3.235	3.053	3.306	3.300	3.299
Fe^{3+}	0.020	0.022	0.026	0.015	0.016
Ti^{4+}	0.001	0.000	0.002	0.000	0.004
total *B*-site	3.256	3.075	3.334	3.315	3.320
Si	0.081	0.172	0.000	0.065	0.079
As	0.003	0.000	0.008	0.000	0.004
Pb	1.913	1.828	1.986	1.929	1.917
S	0.003	0.000	0.006	0.006	0.000
total *T*-site	2.000	2.000	2.000	2.000	2.000
F	2.511	2.420	2.583	2.625	2.412
H	5.745	4.996	5.898	5.882	6.312
OH in (PO_3OH)	1.000	1.000	1.000	1.000	1.000
(OH)	4.745	3.996	4.898	4.882	5.312
(OH)+F	7.256	6.415	7.477	7.506	7.724

Empirical formulas were calculated on the basis of (P+As+Si+S) = 2; all Fe_{tot} as Fe^{3+}; *H_2O content calculated from charge balance.

UNK5 Pb-U oxide/hydroxide – $Pb(UO_2)_3O_3(OH)_2 \cdot 3H_2O$ (?)

UNK5 has been found in several historical specimens (*NMCR*, collected 1949) from Oktyabrskaya vein of the Horní Slavkov uranium ore district (Plášil *et al*. 2006). The phase occurs in uraninite veinlets to 1 cm wide, affected by a strong supergene alteration. Yellow uranophane and phosphuranylite, yellow and yellow-orange

rutherfordine crusts, light yellow-green tabular crystals of autunite and rare nováčekite are the associated minerals. The aggregates of ***UNK5*** are limited to 5 mm long, black relics of hydrated uraninite in altered gangue. The phase usually forms minor veinlets to 0.2 mm wide (Fig. 22) or rare equant aggregates to 0.5 mm, intergrown with black uraninite, yellow uranophane and light yellow-green nováčekite (Fig. 23). ***UNK5*** has a conspicuous orange-red colour, it is transparent, with vitreous lustre and conchoidal fracture.

The X-ray powder diffraction data for ***UNK5*** from Horní Slavkov (Table 11) correspond to data published for an unnamed PbO-UO_3-H_2O phase from the Rovnost mine, Jáchymov (Ondruš *et al.* 1997). The sample from Horní Slavkov contains probably admixture of nováčekite. X-ray powder diffraction data for ***UNK5*** are different from those presented for minerals compositionally related to ***UNK5*** specifically masuyite (Finch – Ewing 1992; Deliens – Piret 1996; Burns – Hanchar 1999) and richetite (Burns 1998).

Quantitative chemical analyses of ***UNK5*** (Table 12) show that the phase is a hydrated oxide/hydroxide of Pb and U with contents of these elements (Fig. 24) close to those of one type of masuyite, reported by Burns – Hanchar (1999), Finch – Ewing (1992) (masuyite I) and Deliens – Piret (1996) ("grooved masuyite"). For this reason, analyses of ***UNK5*** were re-calculated on the basis of U = 3. In contrast to the published masuyite analyses, ***UNK5*** contains minor quantities of other elements (contents expressed as *apfu* fractions): 0.05 Ca, 0.04 K, 0.04 Al, 0.03 Na etc. Based on analogy with masuyite, the empirical formula is $(Pb_{0.81}Ca_{0.04}K_{0.03}Na_{0.02}Mg_{0.01}Al_{0.01})_{\Sigma 0.92}(UO_2)_{3.00}O_3(OH)_{1.67} \cdot 3H_2O$. Figure 24 indicates that the composition of UNK5 is close to the published data for richetite. Recalculation of analyses of the phase from Horní Slavkov on the basis of general formula for richetite proposed by Burns (1998) results in empirical formula $M_{1.61}Pb_{9.69}[(UO_2)_{18}O_{18}(OH)_{10.04}] \cdot 41H_2O$. This formula requires 6.91 wt. % H_2O and the analysis total would be 101.63 wt. %. A problematic question in mineralogy with chemical compositions close to richetite is the occupancy of *M-site* by elements such as Mg, Fe, etc. Burns (1998) derived their content from the crystal structure study as corresponding to 0.47 a 0.83 *apfu* respectively, but microprobe study of identical materi-

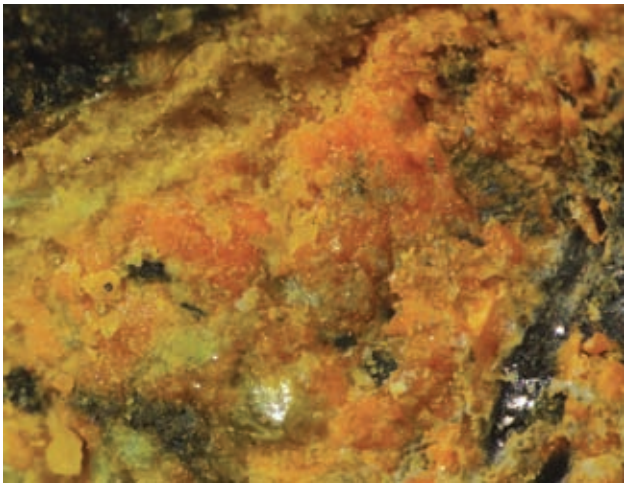

Fig. 22 Orange-red veinlets of ***UNK5*** in black hydrated uraninite with yellow uranophane and greenish nováčekite. Oktyabrskaya vein, Horní Slavkov uranium ore district. Width of the area shown 2 mm. Nikon SMZ1500 photograph by J. Sejkora.

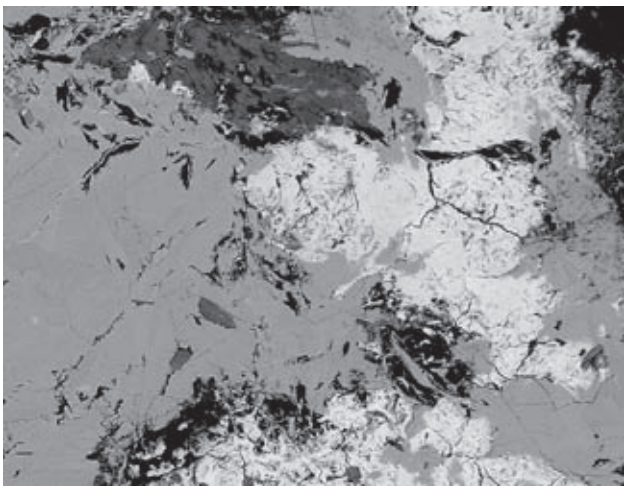

Fig. 23 ***UNK5*** aggregates (light) replacing hydrated uraninite (grey) with nováčekite (dark grey) occurring in cavities and along fractures. Horní Slavkov uranium ore district. Width of the area shown 500 µm. Cameca SX100, BSE photograph by J. Sejkora and R. Škoda.

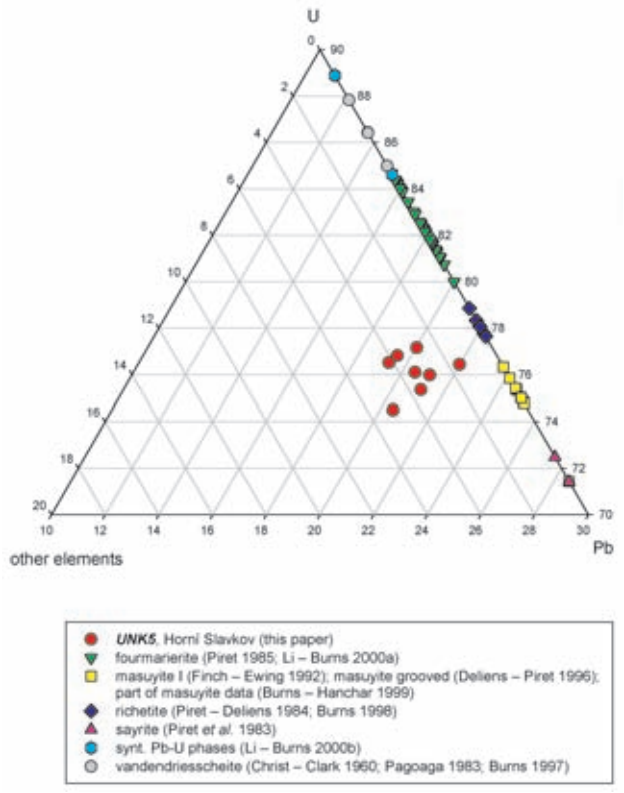

Fig. 24 Part of ternary plot of Pb-U-X in ***UNK5*** from Krásno, compared with published data for other Pb-U-O-H_2O minerals.

Table 11 X-ray powder diffraction pattern of ***UNK5***

I_{rel}	d	I_{rel}*	d*	I_{rel}	d	I_{rel}*	d*	I_{rel}	d	I_{rel}*	d*
		2	16.993	32	3.689	40	3.691	6	2.2504 N	6	2.2557
4	16.293	6	16.155	9	3.607			6	2.2231	4	2.2254
28	10.372	5	10.280	63	3.542 N	44	3.542	6	2.2011	4	2.1995
48	9.981 N			29	3.477	14	3.479	2	2.1691	5	2.1720
46	8.706	9	8.825	11	3.428			7	2.1090	8	2.1068
51	7.994	40	7.907	22	3.358 N	21	3.355	4	2.0866	2	2.0899
82	7.641	100	7.630	14	3.331			4	2.0590	7	2.0668
68	7.230			7	3.272	11	3.277	10	2.0273	10	2.0318
71	7.069	78	7.071	100	3.212	83	3.216	11	1.9922 N	10	2.0205
5	6.733 N			40	3.167 N	21	3.170	19	1.9766	14	1.9790
10	6.367	8	6.354	14	3.094	4	3.099	13	1.9737	9	1.9626
2	6.123			12	3.057			10	1.9475	4	1.9509
21	5.930	12	5.934	18	3.034	9	3.039	1	1.9311	6	1.9315
9	5.707	5	5.705	11	3.009	11	3.004	7	1.9159	18	1.9208
28	5.637	35	5.641	7	2.962			14	1.8900	18	1.8934
3	5.258			22	2.897 N	23	2.901	14	1.8787	7	1.8799
9	5.200			1	2.817	6	2.821	1	1.8554	13	1.8563
10	5.035 N	12	5.005	10	2.762	16	2.763	7	1.8206 N	7	1.8193
19	4.982	4	4.953	7	2.705	11	2.704	12	1.8097	8	1.8121
4	4.765			4	2.641			3	1.8026	13	1.8039
5	4.471	6	4.457	17	2.616	20	2.619	8	1.7961		
8	4.411			10	2.577	6	2.575	6	1.7754 N		
11	4.338	1	4.340			3	2.547	11	1.7450	3	1.7537
		7	4.258	9	2.529 N			6	1.7277	11	1.7221
2	4.168	2	4.174	7	2.505	3	2.509	17	1.7180		
2	4.081	7	4.069	6	2.4918	5	2.4897			4	1.6735
32	3.989	13	3.967	6	2.4311	6	2.4301	3	1.6393	4	1.6424
32	3.929	27	3.924	4	2.3937	2	2.3927	4	1.6089	4	1.6082
26	3.899	38	3.895	11	2.3534	12	3.5510			4	1.5728
7	3.802	10	3.813	5	2.2903	4	2.2893	3	1.5510	5	1.5520

I_{rel}* and d* – unnamed $PbO\text{-}UO_3\text{-}H_2O$ phase (Ondruš *et al.* 1997)
N – probable coincidence with nováčekite

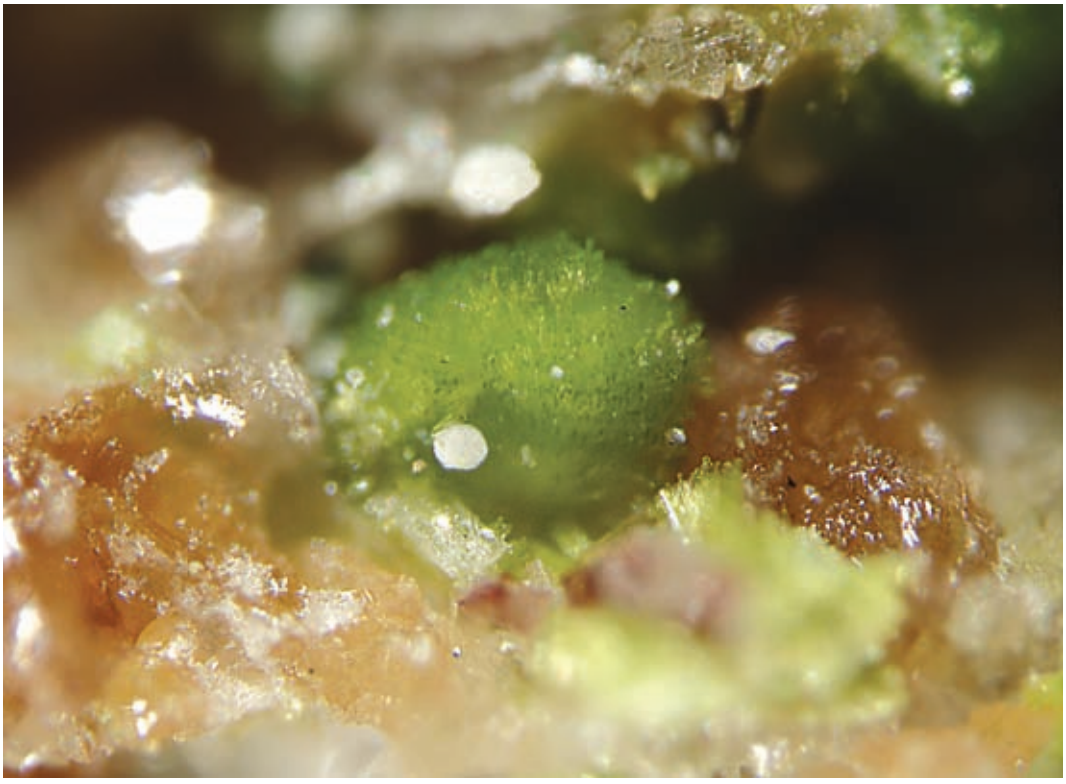

Fig. 25 Radiating aggregates of ***UNK6*** from Huber open pit, Krásno. Width of the area shown 1.5 mm. Nikon SMZ1500 photograph by J. Sejkora.

Table 12 Chemical composition of ***UNK5*** (in wt. %)

	mean	1	2	3	4	5	6	7
Na_2O	0.05	0.06	0.10	0.04	0.04	0.07	0.00	0.01
K_2O	0.11	0.16	0.02	0.16	0.11	0.14	0.14	0.07
CaO	0.19	0.16	0.18	0.11	0.20	0.23	0.27	0.18
FeO	0.04	0.00	0.02	0.06	0.00	0.01	0.22	0.00
BaO	0.02	0.00	0.01	0.03	0.07	0.00	0.03	0.00
MgO	0.04	0.03	0.10	0.06	0.06	0.00	0.06	0.00
PbO	16.25	16.01	16.89	15.41	16.78	15.14	16.60	16.95
CuO	0.06	0.05	0.00	0.18	0.00	0.19	0.00	0.00
ZnO	0.06	0.00	0.17	0.00	0.11	0.07	0.09	0.00
Al_2O_3	0.05	0.03	0.04	0.03	0.00	0.04	0.20	0.03
Bi_2O_3	0.12	0.06	0.09	0.26	0.00	0.24	0.17	0.02
SiO_2	0.19	0.09	0.09	0.00	0.11	0.15	0.44	0.41
As_2O_5	0.02	0.11	0.00	0.04	0.00	0.00	0.03	0.00
P_2O_5	0.02	0.00	0.00	0.02	0.05	0.04	0.00	0.03
V_2O_5	0.03	0.08	0.00	0.00	0.03	0.05	0.00	0.03
SO_3	0.08	0.06	0.00	0.21	0.07	0.03	0.07	0.16
UO_3	77.35	79.04	77.33	77.85	77.42	76.89	77.38	75.53
Cl	0.02	0.06	0.05	0.01	0.00	0.04	0.02	0.00
H_2O*	6.23	6.30	6.39	6.30	6.27	6.17	6.28	5.91
total	100.95	102.28	101.47	100.78	101.31	99.51	101.98	99.31
Na^+	0.016	0.019	0.035	0.013	0.016	0.026	0.000	0.003
K^+	0.027	0.037	0.004	0.038	0.026	0.032	0.032	0.016
Ca^{2+}	0.037	0.031	0.035	0.022	0.039	0.046	0.054	0.036
Fe^{2+}	0.007	0.000	0.003	0.010	0.000	0.001	0.034	0.000
Ba^{2+}	0.002	0.000	0.001	0.002	0.005	0.000	0.002	0.000
Mg^{2+}	0.012	0.007	0.026	0.016	0.015	0.000	0.017	0.000
Pb^{2+}	0.808	0.779	0.840	0.761	0.833	0.757	0.825	0.863
Cu^{2+}	0.008	0.006	0.000	0.025	0.000	0.027	0.000	0.000
Zn^{2+}	0.008	0.000	0.023	0.000	0.014	0.010	0.012	0.000
Al^{3+}	0.012	0.007	0.009	0.006	0.000	0.010	0.043	0.006
Bi^{3+}	0.006	0.003	0.004	0.012	0.000	0.012	0.008	0.001
Si^{4+}	0.034	0.017	0.016	0.000	0.021	0.029	0.080	0.078
As^{5+}	0.002	0.010	0.000	0.003	0.000	0.000	0.003	0.000
P^{5+}	0.003	0.000	0.000	0.004	0.008	0.006	0.000	0.005
V^{5+}	0.003	0.009	0.000	0.000	0.003	0.006	0.000	0.004
S^{6+}	0.012	0.008	0.000	0.029	0.009	0.004	0.009	0.022
U^{6+}	3.000	3.000	3.000	3.000	3.000	3.000	3.000	3.000
Cl^-	0.008	0.017	0.015	0.003	0.000	0.012	0.005	0.001
H^+	7.673	7.593	7.872	7.709	7.715	7.644	7.731	7.454
OH	1.673	1.587	1.871	1.701	1.720	1.647	1.724	1.457
H_2O	3.000	3.003	3.000	3.004	2.997	2.999	3.003	2.999

Mean and spot analyses (1–7). Empirical formulas were calculated on the basis of $(UO_2)^{2+} = 3$; H_2O* content was calculated from the charge balance and ideal content of 3.

al shows that all elements, which potentially could enter the *M-site,* are below the detection limits of the instrument.

UNK6 Cu-Fe phosphate (arthurite group) – $CuFe^{3+}_2(PO_4)_2(OH)_2 \cdot 4H_2O$

UNK6 occurs in several samples of phosphate accumulations from the Huber open pit (Sejkora *et al.* 2006c). Three morphological types of the phase are noted. They also differ in details of their chemical composition and by the associated minerals.

The first type, in the following designated as ***UNK6*** "aggregates", occurs in place of the original triplite accumulations, more than 5 cm in size, which were later altered to brownish fluorapatite, accompanied by lighter compact isokite, and associated with white crystalline quartz. ***UNK6*** is deposited in weathering cavities of mm to 2 cm size. It crystallized on coating of amorphous Fe or Mn-oxides or directly on relics of fresh, brown-red triplite. Small whitish UNK1 aggregates and rare very minute dark green crystals of chalcosiderite – turquoise minerals occur in association with ***UNK6***. The mineral forms abundant radiating to semi-spheroidal aggregates to 1 mm (Fig. 25), composed of thin tabular crystals to 0.5 mm (Figs 26 and 27) and less common crystalline coatings up to several mm^2 in size. The aggregates are bright yellow-green, sometimes with darker green rims and pearly lustre. Individual crystals show a lighter colour, they are translucent to transparent and show intense vitreous lustre.

A second type, designated as ***UNK6*** "crystals", has been found in cavities to 3 cm in size in former triplite accumulations, almost completely altered to compact brown-pink fluorapatite. It is accompanied by abundant translucent leucophosphite crystals, crystals and aggregates of younger fluorapatite, less common crystalline aggregates of a chalcosiderite – turquoise mineral and rare skeletal aggregates of UNK1. ***UNK6*** forms relatively abundant, well-formed long tabular to flat acicular crystals (Fig. 28) up to 0.2 mm long. The crystals tend to form radiating or random groups. The individual ***UNK6*** crystals are transparent to translucent, of predominating yellow-green colour and intense vitreous lustre. Some of the crystals show distinct colour zoning, with lighter (whitmoreite, earlshannonite, UNK8) and darker green (UNK7) parts. ***UNK6*** is sometimes intergrown with colourless to very light yellow-green whitmoreite and darker green UNK7, showing the same crystal morphology as ***UNK6***.

The third type, designated as ***UNK6*** "tables", occurs in a weathering cavity 1 by 1.5 cm in size, in altered phosphate aggregate (fluorapatite, isokite) in association with abundant water-clear crystals of

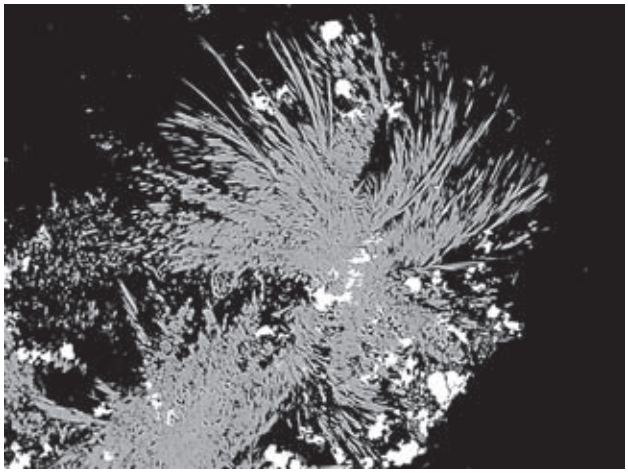

Fig. 26 Radiating agregates of thin tabular ***UNK6*** crystals (grey) with minute chalcopyrite inclusions (light). Width of the area shown 300 μm. Cameca SX100 BSE photograph, by J. Sejkora and R. Škoda.

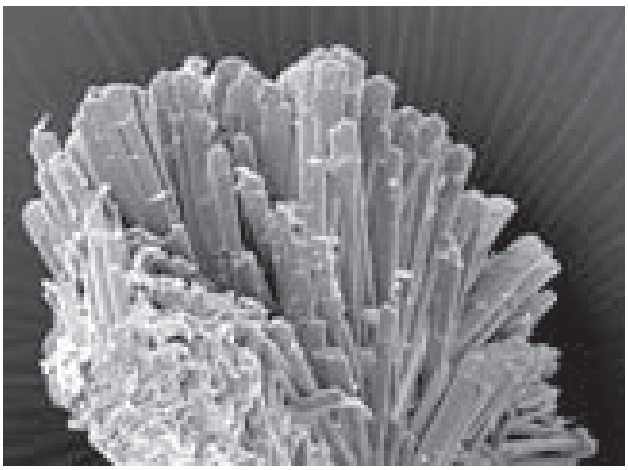

Fig. 27 Radiating agregates of ***UNK6*** crystals, Krásno. Width of the area shown 200 μm. SEM photograph Jeol JSM-6380, J. Sejkora and J. Plášil

younger fluorapatite (sometimes with rutile inclusions), yellow crystals of pharmacosiderite and rare translucent leucophosphite and kolbeckite. In this association, ***UNK6*** forms six-sided tabular aggregates (Fig. 29) up to 0.3 mm long, composed of tabular crystals, which show fibre-like cross-sections (Fig. 30). This type of ***UNK6*** is light green with a yellow tint, aggregates show a limited transparency and a weak mat lustre.

The X-ray data of all three types of ***UNK6*** from Krásno show clear relations of this new phase to the arthurite group. A sample of the type ***UNK6*** "aggregates" was selected for a detailed study, due to the quantity of material available and its chemical homogeneity. The diffraction pattern (Table 13) was indexed using theoretical data calculated from the model of crystal structure for ***UNK6*** (P analogue of arthurite – Keller – Hess 1978). The refined unit-cell parameters of ***UNK6*** (Table 14) are closer to phosphates of the arthurite group than to analogous arsenates. This relation probably reflects the role of anion tetrahedra size: the (PO_4) tetrahedron with bond

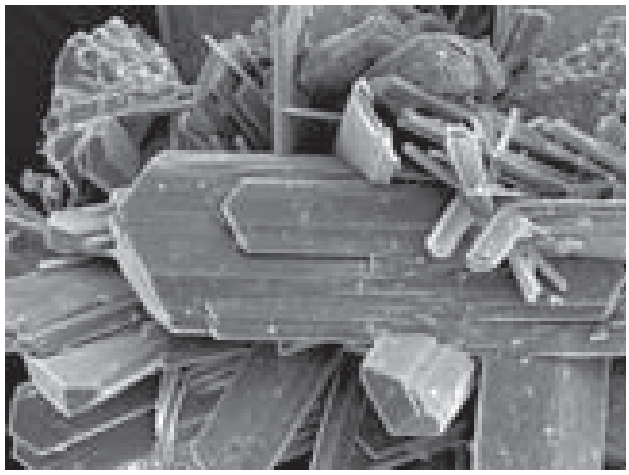

Fig. 28 Elongated tabular to flat acicular ***UNK6*** crystals. Huber open pit, Krásno. Width of the area shown 150 μm. SEM photograph Jeol JSM-6380, J. Sejkora and J. Plášil

Fig. 29 Greenish tabular aggregates of ***UNK6*** in cavity of phoshate accumulation, Huber open pit, Krásno. Width of the area shown 2 mm. Nikon SMZ1500, photograph by J. Sejkora.

Fig. 30 Aggregates of very thin ***UNK6*** tabular crystals (light grey), with kolbeckite crystal (K) and fluorapatite aggregates (darker grey). Width of the area shown 400 μm. Cameca SX100 BSE photograph by J. Sejkora and R. Škoda.

distance of 1.53–1.61 Å (Moore *et al.* 1974) is smaller than (AsO_4) tetrahedron with bond distance of 1.67–1.72 Å (Keller – Hess 1978; Kampf 2005).

Chemical composition of minerals of the arthurite group can be expressed by a general formula $AB_2(TO_4)_2(OH,O)_2 \cdot 4H_2O$ (Table 15). The structural position *A* is occupied mainly by M^{2+} elements, such as Cu, Fe^{2+}, Mn^{2+}, Zn, Co, Mg and Ca (Peacor *et al.* 1984, Jambor *et al*. 2002). According to Moore *et al.* (1974), also Fe^{3+} and vacancies may occur. The study of crystal structure indicates (Keller – Hess 1978, Hughes *et al.* 1996, Kampf 2005) that Cu, Zn and Co enter exclusively the *A*-site. The *B*-site is occupied by dominant Fe^{3+} and some Al^{3+} (Peacor *et al.* 1984, Staněk 1988) and probably minor Ti^{4+} (Staněk 1988). It is also possible that monoclinic kleemanite $ZnAl_2(PO_4)_2(OH)_2 \cdot 3H_2O$ (Pilkington *et al.* 1979) is a member of the arthurite group with dominant Zn-Al-P.

Table 13 X-ray powder diffraction pattern of ***UNK6***

I_{rel}	*d*	*h*	*k*	*l*	I_{rel}	*d*	*h*	*k*	*l*	I_{rel}	*d*	*h*	*k*	*l*
100	9.852	1	0	0	9	2.3975	3	2	1	10	1.8149	0	5	1
35	6.890	1	1	0	10	2.3940	2	3	1	11	1.7481	5	2	-1
73	4.920	2	0	0	13	2.3833	4	1	0	8	1.7146	2	5	-1
24	4.816	0	2	0	9	2.3740	0	2	2	9	1.7043	2	1	-3
7	4.757	0	1	1	12	2.3403	1	4	0	12	1.6986	2	5	1
34	4.380	2	1	0	10	2.3279	1	2	-2	9	1.6826	2	4	2
9	4.326	1	2	0	9	2.2970	3	3	0	11	1.6801	4	2	2
24	4.227	1	1	1	5	2.2833	2	1	2	13	1.6763	5	3	0
20	3.4262	1	2	-1	14	2.2044	0	4	1	5	1.6623	3	5	0
20	3.2788	3	0	0	7	2.1889	4	2	0	5	1.6623	2	1	3
16	3.0591	1	3	0	14	2.1533	4	1	1	11	1.6169	6	1	0
16	2.9489	2	2	-1	11	2.1371	3	3	-1	12	1.6045	5	1	-2
23	2.8763	2	2	1	9	2.1096	2	2	2	7	1.5995	3	4	-2
13	2.7660	0	3	1	12	2.0948	3	3	1	3	1.5739	1	3	-3
35	2.7428	3	1	-1	3	2.0839	0	3	2	4	1.5674	5	0	2
30	2.7063	3	2	0	2	2.0459	1	3	-2	2	1.5630	6	1	-1
27	2.6870	2	3	0	3	2.0283	1	3	2	12	1.5495	1	5	2
13	2.6838	1	3	-1	14	2.0070	4	2	1	12	1.5261	2	6	0
15	2.6584	3	1	1	11	1.9548	3	2	-2	7	1.5198	1	6	1
14	2.6512	1	3	1	19	1.9396	3	4	0	3	1.5131	4	5	0
15	2.6023	1	0	2	7	1.9294	5	1	0	5	1.4935	2	5	2
13	2.5630	1	1	-2	8	1.8939	3	2	2	7	1.4696	4	5	-1
3	2.5179	1	1	2	8	1.8939	1	5	0	10	1.4639	2	6	1
13	2.4562	4	0	0	13	1.8556	4	3	-1	2	1.4560	5	4	1
5	2.4333	2	3	-1	6	1.8377	5	1	-1	7	1.4307	6	0	-2
5	2.4333	2	0	-2	12	1.8298	4	1	-2					
4	2.4085	0	4	0	4	1.8226	5	2	0					

Table 14 Unit-cell parameters of ***UNK6*** (for monoclinic space group $P2_1/c$) and comparison with data for arthurite group minerals

	UNK6	arthurite	ojuelaite	cobaltarthurite	whitmoreite	earlshannonite
	*1	*2	*3	*4	*5	*6
A	Cu	Cu	Zn	Co	Fe	Mn
B	Fe	Fe	Fe	Fe	Fe	Fe
T	P	As	As	As	P	P
a [Å]	9.839(2)	10.189(2)	10.237(1)	10.2635(9)	10.00(2)	9.91(1)
b [Å]	9.636(2)	9.649(2)	9.662(3)	9.7028(8)	9.73(2)	9.669(8)
c [Å]	5.471(1)	5.598(1)	5.562(1)	5.5711(5)	5.471(8)	5.455(9)
ß [°]	92.23(2)	92.16(2)	94.36(1)	94.207(1)	93.8(1)	93.95(9)
V [Å^3]	518.3(1)	549.9(2)	548.5	553.30(8)	531.16	521.4

*1 – Krásno (this paper); *2 – Keller – Hess (1978); *3 Hughes *et al.* (1996); *4 – Kampf (2005); *5 – Moore *et al.* (1974); *6 – Peacor *et al.* (1984).

Table 15 Ideal composition of arthurite group minerals

	A	*B*	*T*	
arthurite	Cu	Fe	As	Davis – Hey (1964)
cobaltarthurite	Co	Fe	As	Jambor *et al.* (2002)
ojuelaite	Zn	Fe	As	Cesbron *et al.* (1981)
earlshannonite	Mn	Fe	P	Peacor *et al.* (1984)
whitmoreite	Fe	Fe	P	Moore *et al.* (1974)
UNK6	Cu	Fe	P	this paper
UNK7	Zn	Fe	P	this paper
UNK8	Fe	Al	P	this paper

The anion tetrahedral *T* position may contain minor S and Si, next to the dominating As and P. Davis – Hey (1969) found 0.40 *apfu* P and 0.22 *apfu* S besides 1.38 *apfu* As in arthurite; Jambor *et al.* (2002) reported P contents to 0.04 *apfu* and S to 0.01 *apfu* for cobaltarthurite. Frost *et al.* (2003) found 0.55 *apfu* As and 1.46 *apfu* P in arthurite from Hingston Down, Consols Mine, Calstock, Cornwall (Great Britain). According to these data, the relation is obviously P>As and this mineral should

Table 16 Chemical composition of ***UNK6*** (in wt. %)

	aggregates					crystals				tables			
	mean	1	2	3	4	mean	5	6	7	mean	8	9	10
Na_2O	0.01	0.00	0.00	0.06	0.00	0.03	0.04	0.00	0.00	0.00	0.00	0.00	
K_2O	0.01	0.02	0.00	0.00	0.02	0.02	0.05	0.04	0.00	0.00	0.00	0.00	
CuO	21.04	20.80	20.36	20.06	21.82	18.03	19.29	18.00	15.91	21.36	20.27	22.32	16.88
MnO	0.02	0.00	0.13	0.00	0.00	0.02	0.00	0.00	0.00	0.01	0.02	0.00	
ZnO	0.54	0.22	0.84	0.90	0.95	1.11	1.08	0.28	1.00	0.28	0.19	0.26	
BaO	0.00	0.00	0.00	0.00	0.00	0.06	0.22	0.00	0.00	0.00	0.00	0.00	
CaO	0.08	0.05	0.03	0.04	0.11	0.53	0.31	0.03	0.03	0.05	0.05	0.07	
PbO	0.01	0.07	0.00	0.03	0.05	0.05	0.00	0.00	0.00	0.06	0.03	0.16	
MgO	0.04	0.08	0.00	0.10	0.11	0.12	0.01	0.08	0.25	0.00	0.00	0.00	
FeO*	0.00	0.00	0.00	0.00	0.00	0.00	0.00	0.02	0.42	0.00	0.00	0.00	
Fe_2O_3*	29.68	30.13	30.75	30.11	30.28	34.53	32.75	36.26	35.81	29.86	29.64	31.06	33.88
Al_2O_3	0.39	0.25	0.34	0.43	0.57	1.07	2.74	0.52	0.25	0.46	0.44	0.42	
SiO_2	0.04	0.07	0.08	0.00	0.03	0.04	0.11	0.00	0.00	0.04	0.02	0.07	
TiO_2	0.00	0.00	0.00	0.00	0.00	0.21	0.51	0.00	0.00	0.00	0.00	0.00	
As_2O_5	10.66	16.81	6.74	5.46	3.70	5.95	1.64	10.43	7.26	21.58	20.49	22.55	
P_2O_5	22.99	19.31	26.17	26.99	28.55	29.01	33.09	26.51	27.70	14.43	14.71	14.95	30.12
SO_3	0.01	0.05	0.00	0.04	0.03	0.01	0.00	0.00	0.00	0.05	0.00	0.03	
H_2O**	18.71	18.33	19.02	19.05	19.24	19.71	20.12	19.39	19.50	18.20	18.20	18.26	19.12
total	104.23	106.19	104.47	103.27	105.47	110.49	111.96	111.55	108.14	106.37	104.05	110.15	100.00
Na	0.002	0.000	0.000	0.009	0.000	0.004	0.005	0.000	0.000	0.000	0.000	0.000	
K	0.001	0.002	0.000	0.000	0.002	0.002	0.005	0.004	0.000	0.000	0.000	0.000	
Σ M^{1+}	0.002	0.002	0.000	0.009	0.002	0.007	0.010	0.004	0.000	0.000	0.000	0.000	
Ca	0.007	0.004	0.003	0.003	0.009	0.041	0.023	0.003	0.003	0.004	0.005	0.006	
Fe^{2+}	0.000	0.000	0.000	0.000	0.000	0.000	0.000	0.001	0.026	0.000	0.000	0.000	
Ba	0.000	0.000	0.000	0.000	0.000	0.002	0.006	0.000	0.000	0.000	0.000	0.000	
Mg	0.005	0.009	0.000	0.011	0.012	0.013	0.001	0.008	0.027	0.000	0.000	0.000	
Pb	0.000	0.002	0.000	0.001	0.001	0.001	0.000	0.000	0.000	0.001	0.001	0.003	
Cu	1.267	1.245	1.194	1.177	1.260	0.982	1.005	0.975	0.882	1.368	1.321	1.374	1.000
Mn	0.001	0.000	0.009	0.000	0.000	0.001	0.000	0.000	0.000	0.000	0.001	0.000	
Zn	0.032	0.013	0.048	0.052	0.054	0.059	0.055	0.015	0.054	0.017	0.012	0.015	
Σ A	1.312	1.273	1.254	1.244	1.336	1.099	1.090	1.002	0.992	1.392	1.340	1.399	1.000
Al^{3+}	0.037	0.023	0.031	0.039	0.052	0.091	0.222	0.044	0.022	0.045	0.045	0.041	
Fe^{3+}	1.781	1.797	1.796	1.761	1.742	1.875	1.701	1.956	1.978	1.906	1.924	1.905	1.999
Ti^{4+}	0.000	0.000	0.000	0.000	0.000	0.011	0.027	0.000	0.000	0.000	0.000	0.000	
Σ B	1.817	1.820	1.828	1.800	1.793	1.978	1.950	2.000	2.000	1.952	1.969	1.946	1.999
Si	0.003	0.006	0.006	0.000	0.002	0.003	0.008	0.000	0.000	0.004	0.002	0.005	
As	0.444	0.696	0.274	0.222	0.148	0.225	0.059	0.391	0.279	0.957	0.924	0.961	
P	1.552	1.295	1.720	1.776	1.848	1.772	1.933	1.609	1.721	1.036	1.074	1.031	2.000
S	0.001	0.003	0.000	0.002	0.002	0.001	0.000	0.000	0.000	0.003	0.000	0.002	
Σ T	2.000	2.000	2.000	2.000	2.000	2.000	2.000	2.000	2.000	2.000	2.000	2.000	2.000
H	10.076	9.995	9.987	9.899	10.049	10.154	10.066	10.008	9.982	10.646	10.588	10.652	9.999
OH	2.076	2.005	1.985	1.899	2.053	2.146	2.059	2.007	1.984	2.638	2.585	2.631	1.999
H_2O	4.000	3.995	4.001	4.000	3.998	4.004	4.003	4.001	3.999	4.004	4.001	3.997	4.000

Empirical formulas were calculated on the basis of (P+As+Si+S) = 2;
* calculation of Fe_{tot} to Fe^{2+} and Fe^{3+} is based on the assumption that Fe^{3+} (jointly with Al^{3+} and Ti^{4+}) preferentially occupied the B^{3+} position; only Fe in surplus, above 2 *apfu,* enters the A^{2+} position as Fe^{2+} ; **H_2O content calculated on the basis of the general formula (H_2O = 4) and charge balance. 1–9 – selected spot analyses of ***UNK6***, 10 – theoretical composition calculated from the formula $CuFe^{3+}_2(PO_4)_2(OH)_2 \cdot 4H_2O$.

correspond to *UNK6*. However, the data reported by Frost *et al.* (2003) can be considered only as preliminary with regard to ED analysis, problems in stoichiometry, discrepancies in systematics, etc.

Chemical composition of all ***UNK6*** types from Krásno is presented in Table 16 and in Figs 31–33. The high analytical totals in the range of 103–112 wt.%, after inclusion of the theoretical H_2O content, indicate partial dehydration of the samples studied in vacuum and their instability under electron beam. The differences in totals of the analyzed ***UNK6*** samples correlate with the diameter of electron beam in individual analyses and do not indicate true differences in chemical composition of the studied mineral phase. *A*-site in ***UNK6*** "aggregates" is dominated by Cu (1.12–1.40 *apfu*) and contains Zn (0.01–0.05 *apfu*) and variable contents of Ca (max. 0.02 *apfu*) and Na, Mg (max. 0.01 *apfu*). The composition of *A*-site of ***UNK6*** "tables" is similar to the first type: Cu (1.32–1.39 *apfu*), Zn (0.01–0.03 *apfu*) and Ca (max. 0.01 *apfu*). The composition of *A*-site of ***UNK6*** "crystals" is variable (Fig. 31). In addition to dominant Cu (0.82–1.32 *apfu*), there are Zn (0.01–0.13 *apfu*) and variable contents of Fe (max. 0.12 *apfu*), Ca, Mg (max. 0.04 *apfu*) and Na (max. 0.01 *apfu*).

The *B*-sites (Fig. 32) of ***UNK6*** "aggregates" and "tables" contain Fe^{3+} (1.59–1.97; 1.89–1.92 *apfu*) and Al (0.02–0.06 and 0.04–0.05 *apfu,* respectively). ***UNK6*** "crystals" contain besides Fe^{3+} (1.64–1.98 *apfu*), minor Ti (max. 0.04 *apfu*), and Al. The content of the latter varies in two ranges – 0.02 to 0.07 and 0.20 to 0.23 *apfu*. The tetrahedral *T*-site of ***UNK6*** "aggregates" and "crystals" (Fig. 33) contain dominant P (1.26–1.93 *apfu*), As (0.06–0.74 *apfu*) and minor Si (max. 0.01 *apfu*). In ***UNK6*** "tables" P (1.01–1.07 *apfu*) just slightly predominates over As (0.92–0.99 *apfu*).

The average empirical formula of ***UNK6*** "aggregates" (18 spot analyses) is $(Cu_{1.27}Zn_{0.03}Ca_{0.01}Mg_{0.01})_{\Sigma 1.32}(Fe_{1.78}Al_{0.04})_{\Sigma 1.82}[(PO_4)_{1.55}(AsO_4)_{0.44}]_{\Sigma 1.99}(OH)_{2.08} \cdot 4H_2O$; the average formula of ***UNK6*** "crystals" (19 spot analyses) is

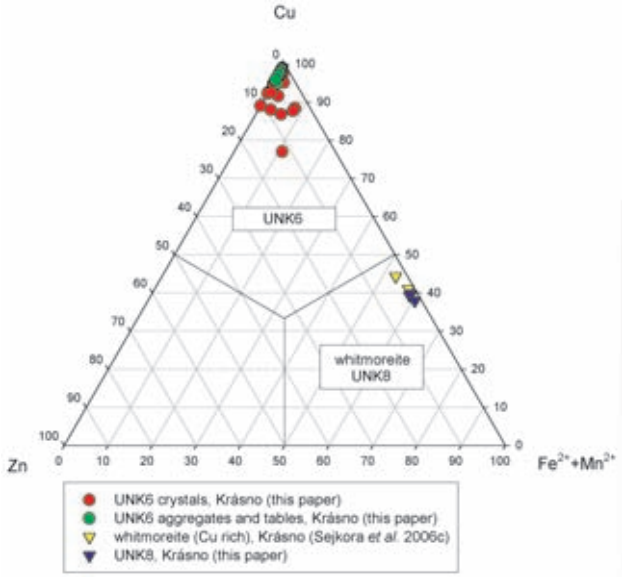

Fig. 31 Ternary plot Cu-Zn-(Fe^{2+}+Mn^{2+}) of *A*-site occupancy (atomic ratios) for arthurite group mineral phases (***UNK6***, ***UNK8***, Cu-rich whitmoreite) from Krásno.

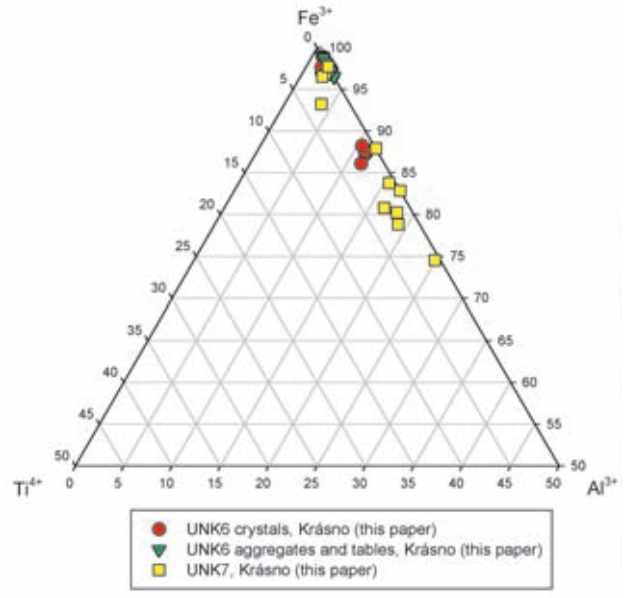

Fig. 32 Part of ternary plot Fe^{3+}-Ti-Al of *B*-site occupancy (atomic ratios) for arthurite group mineral phases (***UNK6***, ***UNK7***) from Krásno

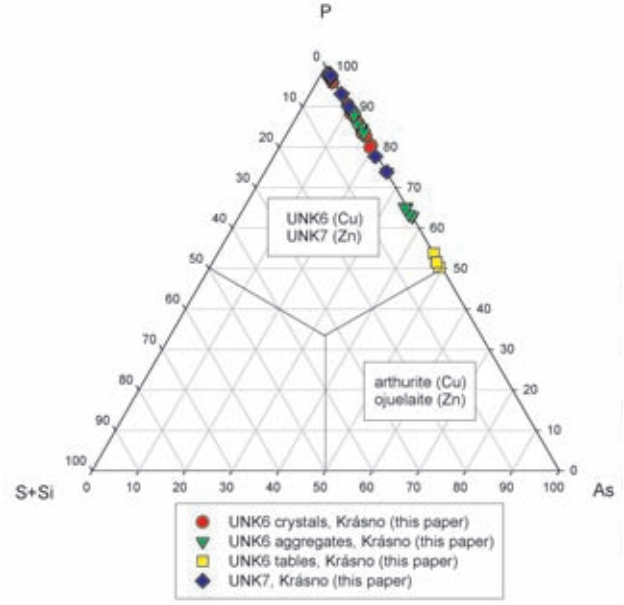

Fig. 33 Ternary plot P-(S+Si)-As of *T*-site occupancy (atomic ratios) for arthurite group mineral phases (***UNK6***, ***UNK7***) from Krásno.

$(Cu_{0.98}Zn_{0.06}Ca_{0.04}Mg_{0.01})_{\Sigma 1.09}(Fe_{1.88}Al_{0.09}Ti_{0.01})_{\Sigma 1.98}[(PO_4)_{1.77}(AsO_4)_{0.23}]_{\Sigma 2.00}(OH)_{2.15} \cdot 4H_2O$; the formula for ***UNK6*** "tables" (4 spot analyses) is $(Cu_{1.37}Zn_{0.02})_{\Sigma 1.39}(Fe_{1.91}Al_{0.05})_{\Sigma 1.96}[(PO_4)_{1.04}(AsO_4)_{0.96}]_{\Sigma 2.00}(OH)_{2.64} \cdot 4H_2O$.

UNK7 Zn-Fe phosphate (arthurite group) $ZnFe^{3+}_2(PO_4)_2(OH)_2 \cdot 4H_2O$

The phase ***UNK7*** has been found in samples collected in the Huber open pit. It occurs in cavities 2–3 cm in diameter in former accumulations of triplite, almost completely altered to pink-brown fluorapatite (Sejkora *et al.* 2006c). ***UNK7*** is associated with abundant translucent leucophosphite crystals, whitish crystals and aggregates of younger fluorapatite, abundant small, yellow-green crystals of UNK6, less common crystals of chalcosiderite-turquoise minerals, very rare snow-white skeletal crystals of UNK1 and colourless to very light yellow-green crystals of whitmoreite. Individual crystals of ***UNK7***, maximum 0.1 mm in size, are elongated-tabular, lath-shaped, transparent to translucent, usually green with an intense vitreous lustre. Crystal morphology of this material is indistinguishable from those of UNK6 and whitmoreite. Green prismatic ***UNK7*** crystals (max. 0.1 mm) with uneven surface and greasy lustre are rare. The ***UNK7*** phase shows, in parts of some crystals, colour zoning, including yellow-green (UNK6) and lighter domains (whitmoreite, earlshannonite, UNK8).

Owing to the very small size of ***UNK7***, it was not possible to identify it by X-ray powder diffraction. Its classification with the arthurite group is based on stoichiometry of chemical composition and the occurrence as individual zones in the zoned crystals of the arthurite group minerals.

The chemical composition of minerals of the arthurite group can be expressed by a general formula $AB_2(TO_4)_2(OH,O)_2 \cdot 4H_2O$. A detailed discussion of occupancy of the individual structure sites is discussed with the phase UNK6. Variation in totals of the individual spot analyses of ***UNK7*** in the range of 94–109 wt. % (after inclusion of calculated H_2O content) is caused mainly by variable diameter of the electron beam, selected in dependence of variable size of individual domains in the zoned crystals (Table 17).

Zn (0.35–0.75 *apfu*) is the dominant cation in *A*-site of ***UNK7*** (Fig. 34). Fe^{2+} contents are also significant (0.17–0.44 *apfu*), while Mn^{2+} (0–0.09, rarely up to 0.27 *apfu*), Mg (max. 0.16 *apfu*), Na (max. 0.09 *apfu*) and Ca (max. 0.04 *apfu*) represent minor elements. The content of Cu in *A*-site of ***UNK7*** is only 0.04 *apfu*, in conformity with the two observed trends of isomorphism in the arthurite group. These are the Cu-Fe-Mn and Zn-Fe-Mn trends, with limited substitution Cu-Zn. In the *B*-site (Fig. 32), in addition to dominating Fe^{3+} (1.49 to 1.95 *apfu*), aluminium (Al max. 0.49 *apfu*) and minor Ti to 0.06 apfu is present. The tetrahedral *T*-site is dominated by P in the range of 1.48–1.96 apfu, in part substituted by As (0.03–0.52 *apfu*) and invariable minor Si and S contents (Fig. 33). The empirical formula for the phase ***UNK7*** (average of 11 spot analyses), calculated on the basis of T = 2, is $(Zn_{0.61}Fe^{2+}_{0.33}Na_{0.06}Mn_{0.05}Ca_{0.03}Cu_{0.02})_{\Sigma 1.10}(Fe^{3+}_{1.73}Al_{0.25}Ti_{0.02})_{\Sigma 2.00}[(PO_4)_{1.86}(AsO_4)_{0.14}]_{\Sigma 2.00}(OH)_{2.25} \cdot 4H_2O$.

Table 17 Chemical composition of ***UNK7*** (in wt. %)

	mean	1	2	3	4	5	6
Na_2O	0.41	0.12	0.32	0.25	0.58	0.61	
K_2O	0.02	0.00	0.00	0.00	0.00	0.11	
CuO	0.38	0.10	0.74	0.00	0.26	0.14	
MnO	0.78	4.02	0.00	0.10	0.00	0.39	
ZnO	10.95	6.03	8.16	7.49	12.04	13.12	17.20
BaO	0.02	0.01	0.00	0.06	0.00	0.07	
SrO	0.01	0.00	0.00	0.05	0.00	0.00	
CaO	0.33	0.24	0.07	0.08	0.35	0.42	
MgO	0.37	1.00	1.43	0.14	0.01	0.07	
FeO*	5.27	2.93	4.57	5.16	7.24	5.85	
Fe_2O_3*	30.44	32.48	34.72	28.74	32.09	29.09	33.75
Al_2O_3	2.80	0.52	0.52	0.75	2.82	3.80	
SiO_2	0.04	0.10	0.00	0.00	0.00	0.09	
TiO_2	0.40	0.24	0.00	0.91	0.00	0.96	
As_2O_5	3.46	10.52	3.45	11.58	1.21	0.86	
P_2O_5	29.12	23.19	29.45	20.25	31.71	31.37	30.00
H_2O**	20.00	19.30	19.92	18.78	20.22	20.32	19.04
total	104.81	100.80	103.35	94.34	108.51	107.27	100.00
Na	0.060	0.019	0.047	0.042	0.082	0.088	
K	0.002	0.000	0.000	0.000	0.000	0.010	
Ca	0.027	0.020	0.006	0.007	0.028	0.033	
Fe^{2+}	0.332	0.194	0.286	0.372	0.441	0.361	
Ba	0.001	0.000	0.000	0.002	0.000	0.002	
Sr	0.000	0.000	0.000	0.002	0.000	0.000	
Mg	0.041	0.118	0.160	0.018	0.001	0.007	
Cu	0.021	0.006	0.042	0.000	0.014	0.008	
Mn	0.050	0.270	0.000	0.007	0.000	0.025	
Zn	0.610	0.353	0.451	0.477	0.647	0.715	1.000
A total	1.144	0.981	0.990	0.928	1.212	1.249	1.000
Al^{3+}	0.249	0.049	0.046	0.076	0.242	0.331	
Fe^{3+}	1.728	1.937	1.954	1.864	1.758	1.616	1.999
Ti^{4+}	0.023	0.014	0.000	0.059	0.000	0.053	
B total	2.000	2.000	2.000	2.000	2.000	2.000	1.999
Si	0.003	0.008	0.000	0.000	0.000	0.007	
As	0.137	0.436	0.135	0.522	0.046	0.033	
P	1.860	1.556	1.865	1.478	1.954	1.960	2.000
T total	2.000	2.000	2.000	2.000	2.000	2.000	2.000
H	10.243	9.954	9.926	9.878	10.339	10.440	9.999
OH	2.248	1.949	1.933	1.873	2.342	2.446	1.999
H_2O	3.997	4.002	3.996	4.003	3.999	3.997	4.000

Empirical formulas were calculated on the basis of (P+As+Si+S) = 2; 1–5 – representative analyses and mean of 11 spot analyses of ***UNK7***; 6 – theoretical composition calculated from the formula $ZnFe^{3+}_2(PO_4)_2(OH)_2 \cdot 4H_2O$.

* calculation of Fe_{tot} to Fe^{2+} and Fe^{3+} is based on the assumption that Fe^{3+} preferentially (together with Al^{3+} and Ti^{4+}) occupied the position B^{3+} and only the surplus Fe (above 2 *pfu*) enters the position A^{2+} as Fe^{2+}.

** H_2O content calculated from the general formula (H_2O = 4) and charge balance.

UNK8 FeAl phosphate (arthurite group) $Fe^{2+}Al^{3+}_2(PO_4)_2(OH)_2 \cdot 4H_2O$

UNK8 has been identified in cavities 2–3 cm in diameter in former triplite accumulations, nearly completely altered to compact pink-brown fluorapatite from the Huber open pit (Sejkora *et al.* 2006c). It associates with

abundant leucophosphite, fluorapatite, UNK6, less common UNK7, minerals of the chalcosiderite-turquoise series, exceptional whitmoreite and UNK1. ***UNK8*** was observed as a single irregular zone 30 by 40 μm in size, in a UNK6 crystal. Owing to the minimal dimensions, the phase could not be studied by X-ray powder diffraction. Its classification with the arthurite group is based on stoichiometry of chemical composition and intergrowth with UNK6.

The chemical composition of minerals of the arthurite group can be expressed by a general formula $AB_2(TO_4)_2(OH,O)_2 \cdot 4H_2O$. A detailed discussion of occupancy of the individual structure sites is discussed with the phase UNK6. Variation in totals of the individual spot analyses of ***UNK8*** in the range of 94–106 wt. % (after inclusion of calculated H_2O content) indicate dehydration of the studied sample in vacuum and its instability under electron beam (Table 18). The *A*-site in ***UNK8*** (Fig. 31) is dominated by Fe^{2+} (0.88–1.02 *apfu*), accompanied by Cu (0.60–0.65 *apfu*), minor Zn (max. 0.03 *apfu*), and Ca (max. 0.01 *apfu*). The dominant element in the *B*-site (Fig. 35) is Al (1.59–1.97) *apfu* and Fe^{3+} (max. 0.37 *apfu*), and minor Ti (max. 0.04 *apfu*). The tetrahedral *T*-site (Fig. 36) is nearly completely occupied by

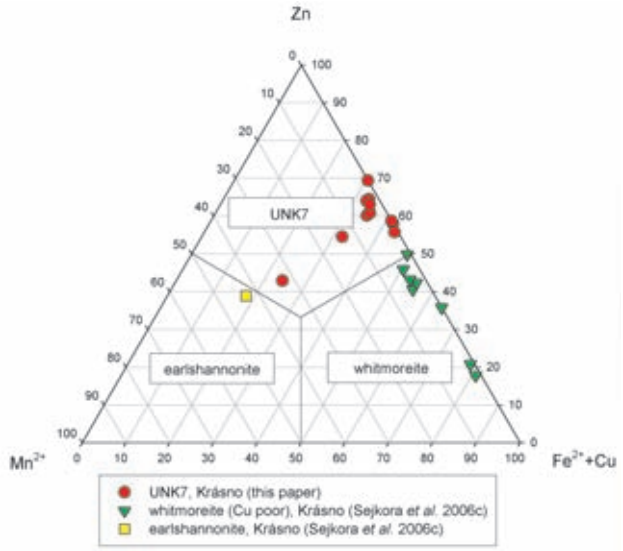

Fig. 34 Ternary plot of Zn-Mn^{2+}–(Fe^{2+}+Cu) occupancy of *A*-site (atomic ratios) for arthurite group mineral phases (***UNK7***, earlshannonite and Cu-poor whitmoreite) from Krásno.

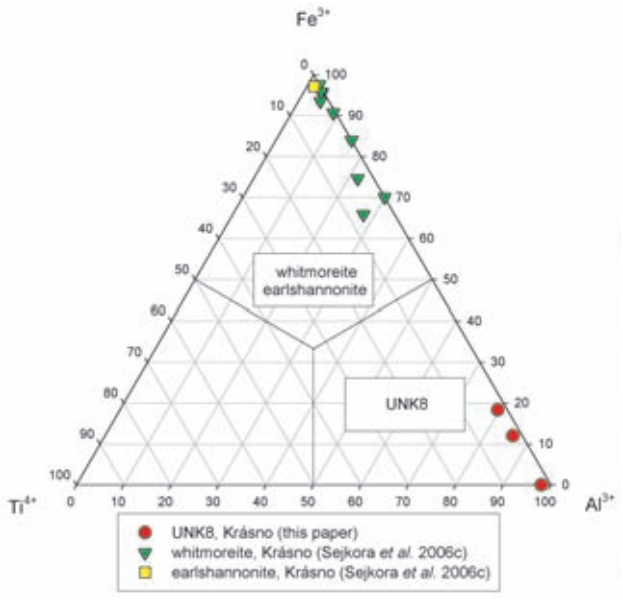

Fig. 35 Ternary plot Fe^{3+}-Ti-Al of *B*-site occupancy (atomic ratios) for arthurite group mineral phases (***UNK8***, whitmoreite and earlshannonite) from Krásno.

Table 18 Chemical composition of ***UNK8*** (in wt. %)

	mean	1	2	3	4
Na_2O	0.01	0.00	0.04	0.00	
K_2O	0.08	0.11	0.05	0.08	
CuO	11.10	10.64	11.19	11.48	
MnO	0.04	0.09	0.00	0.02	
ZnO	0.50	0.43	0.61	0.48	
BaO	0.10	0.04	0.25	0.02	
SrO	0.10	0.17	0.12	0.02	
CaO	0.14	0.11	0.19	0.12	
PbO	0.03	0.00	0.10	0.00	
FeO*	15.23	14.12	15.07	16.38	17.70
Fe_2O_3*	3.54	6.53	4.23	0.00	
Al_2O_3	19.92	18.12	19.33	22.32	25.12
SiO_2	0.03	0.06	0.03	0.00	
TiO_2	0.71	0.72	0.70	0.72	
As_2O_5	0.50	0.57	0.36	0.56	
P_2O_5	31.17	31.25	31.02	31.24	34.97
H_2O**	21.64	21.50	21.58	21.90	22.20
total	104.86	104.46	104.86	105.32	100.00
Na	0.002	0.000	0.005	0.000	
K	0.008	0.010	0.005	0.008	
Ca	0.011	0.009	0.015	0.009	
Fe^{2+}	0.955	0.881	0.952	1.024	1.000
Ba	0.003	0.001	0.007	0.001	
Sr	0.004	0.007	0.005	0.001	
Pb	0.001	0.000	0.002	0.000	
Cu	0.629	0.600	0.638	0.648	
Mn	0.002	0.006	0.000	0.001	
Zn	0.028	0.023	0.034	0.026	
A total	1.642	1.536	1.665	1.719	1.000
Al^{3+}	1.760	1.593	1.720	1.968	2.000
Fe^{3+}	0.200	0.367	0.240	0.000	
Ti^{4+}	0.040	0.040	0.039	0.040	
B total	2.000	2.000	2.000	2.008	2.000
Si	0.002	0.004	0.003	0.000	
As	0.019	0.022	0.014	0.022	
P	1.978	1.973	1.983	1.978	2.000
T total	2.000	2.000	2.000	2.000	2.000
H	11.308	11.102	11.354	11.507	10.000
OH	3.313	3.099	3.356	3.509	2.000
H_2O	3.997	4.002	3.999	3.999	4.000

Empirical formulas are calculated on the basis of (P+As+Si+S) = 2;
Average composition and 1, 2, 3 – spot analyses of ***UNK8***;
4 – theoretical composition calculated from the formula $Fe^{2+}Al^{3+}_2(PO_4)_2(OH)_2 \cdot 4H_2O$.
* calculation of Fe_{tot} to Fe^{2+} and Fe^{3+} is based on the assumption that Fe^{3+} preferentially (together with Al^{3+} and Ti^{4+}) occupied the position B^{3+} and only the surplus Fe (above 2 *pfu*) enters the position A^{2+} as Fe^{2+}.
** H_2O content calculated from the general formula (H_2O = 4) and charge balance.

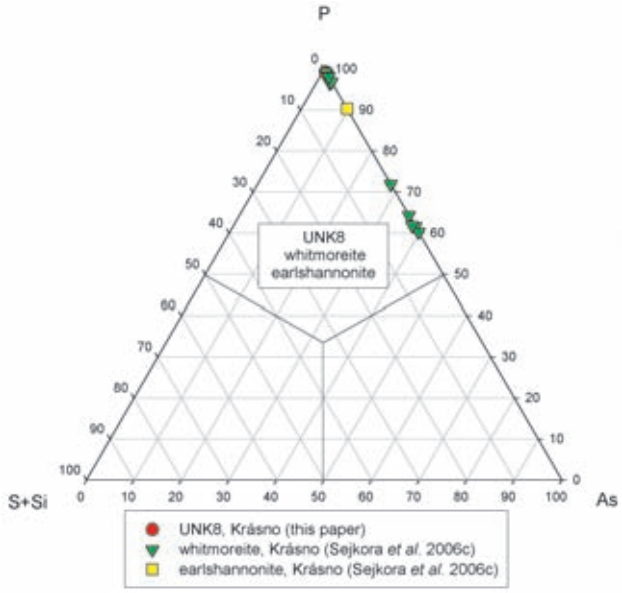

Fig. 36 Ternary plot P-(S+Si)-As of *T*-site occupancy (atomic ratios) for arthurite group mineral phases (***UNK8***, whitmoreite and earlshannonite) from Krásno.

P (1.97–1.98 *apfu*) with minor substitution of As in the range of 0.01 to 0.02 *apfu*. The empirical formula of ***UNK8*** (average of three spot analyses) on the basis T = 2.00 is $(Fe^{2+}_{0.96}Cu_{0.63}Zn_{0.03}Ca_{0.01})_{\Sigma 1.63}(Al_{1.76}Fe^{3+}_{0.20}Ti_{0.04})_{\Sigma 2.00}[(PO_4)_{1.98}(AsO_4)_{0.02})_{\Sigma 2.00}(OH)_{3.31} . 4H_2O$

UNK9 Fe-Mn phosphate – $(Mn^{2+},Fe^{2+})_2(Fe^{3+},Al)_3(PO_4)_3(OH)_4 . H_2O$

UNK9 is fairly abundant in several samples of phosphate accumulations collected at the 5th level of the Huber shaft (Sejkora *et al.* 2006c). It occurs in parts where triplite is nearly completely replaced by younger minerals of the rockbridgeite – frondelite series. These black phosphates with greenish or brownish shade are in turn partly altered, giving rise to aggregates of blue-grey phosphosiderite. In some specimens, ***UNK9*** is younger than phosphosiderite, in other specimens it is older, as it is overgrown by younger phosphosiderite. The youngest minerals in this association are light pink morinite, beraunite grains and purple-red strengite, acicular crystals of natrodufrénite and compact aggregates of K-Mn oxide enclosing semispheroidal fluorite.

UNK9 typically occurs as light to dark brown tabular aggregates of crystals (Fig. 37), 2–3 mm in size, in minor cavities 2 to 3 mm in diameter. The aggregates are composed of imperfect (Figs 38 and 39) transparent, tabular to scaly crystals up to 0.5 mm long, with a vitreous to pearly lustre. The phase has a yellow-brown streak with a slight green shade.

X-ray powder data for ***UNK9*** from Krásno (Table 19) correspond well to data for the unnamed Fe-Mn "dufrénite-like" mineral from Buranga, Rwanda (Knorring – Sahama 1982). However, it is not possible to index X-ray powder diffraction data correctly on the basis of

Fig. 37 Dark brown crystalline aggregates of ***UNK9***, Krásno. Width of the area shown 3.5 mm. Nikon SMZ1500, photograph by J. Sejkora.

Table 19 X-ray powder diffraction pattern of ***UNK9***

I_{rel}	d	I_{rel}*	d*	I_{rel}	d	I_{rel}*	d*	I_{rel}	d	I_{rel}*	d*
71	6.916	40	6.93	87	3.016	60	3.020	40	2.1154	20	2.120
		20	6.43	33	2.942	20	2.950	28	2.0700	20	2.080
13	5.185	40	5.22	9	2.879	20	2.880	36	2.0301	20	2.040
17	4.843	60	4.86	42	2.806	20	2.820	7	1.9820	20	1.980
14	4.363	20	4.43	10	2.764	20	2.750	36	1.9432	40	1.950
35	4.231	40	4.23	27	2.701			10	1.8812	20	1.880
56	4.021	20	4.03	66	2.625	60	2.630	9	1.8506	20	1.850
29	3.883	20	3.88	12	2.504	10	2.510			20	1.820
42	3.730	40	3.734	11	2.4466	60	2.440	26	1.7855	20	1.790
98	3.447	100	3.464	19	2.2829	20	2.300	29	1.7417	20	1.750
91	3.263	80	3.264			20	2.220	56	1.7227	40	1.730
100	3.212	80	3.218	35	2.1761	20	2.180				
33	3.148	60	3.151	14	2.1552	20	2.150				

I_{rel}* and d* – unnamed mineral (dufrénite-like), Buranga, Rwanda (Knorring – Sahama, 1982).

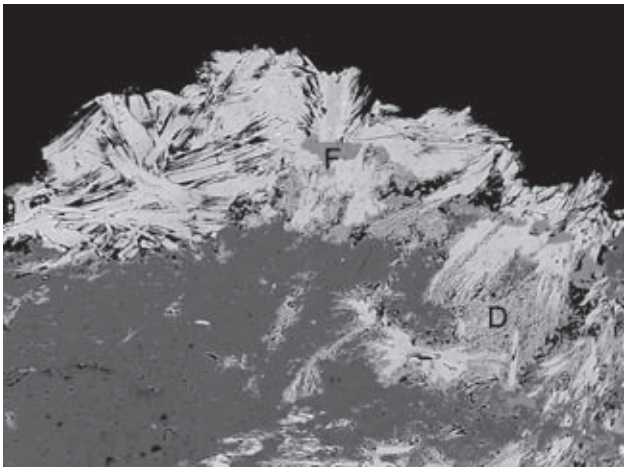

Fig. 38 Aggregates of tabular crystals of ***UNK9*** (light) deposited on phosphosiderite aggregate (dark), accompanied by granular fluorapatite (F) and finely fibrous Mn-rich dufrenite (D) aggregates. Width of the area shown 500 μm. Cameca SX100, BSE photograph by J. Sejkora and R. Škoda.

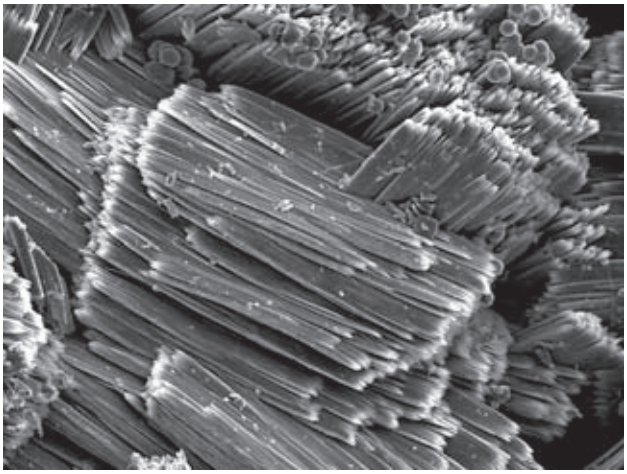

Fig. 39 Group of tabular ***UNK9*** crystals, Krásno. Width of the area shown 180 μm. SEM photograph Jeol JSM-6380, J. Sejkora and J. Plášil.

monoclinic unit-cell parameters (a= 6.44(2), b=6.93(2), c=19.43(3), ß=93.25°) proposed by Knorring – Sahama (1982). However, it should be noted that the X-ray powder data for ***UNK9*** show closer relations to those of the rockbridgeite – frondelite series than to published data for dufrénite-like minerals (dufrénite, natrodufrénite, burangaite).

Knorring – Sahama (1982) published for the phase from Buranga, analogous to ***UNK9***, chemical analysis of major elements but did not present empirical formula. On the basis of coincidence of the X-ray powder data (of poor quality) with an unnamed "dufrénite-like" Fe phosphate, which was not analyzed (Frondel 1949), from Rothläufchen mine (Germany), they suggested that the mineral is close to dufrénite. An unnamed author of the entry No. 35–725 in the data-base of X-ray powder patterns PDF2 gave for this unnamed phosphate an ideal formula $(Fe,Mn)_5(PO_4)_3(OH)_5 \cdot 2H_2O$, in analogy to the dufrénite formula proposed by Frondel (1949). However, a characteristic feature of dufrénite-like minerals (dufrénite, natrodufrénite, burangaite) is the presence of Na, K and Ca, not previously discussed. In addition to differences in chemical composition, ***UNK9*** differs from dufrénite-like minerals by X-ray diffraction pattern.

We believe that it is appropriate to express the chemical composition of ***UNK9*** (Table 20) by a general formula $A_2B_3(PO_4)_3(OH)_4 \cdot H_2O$. It is assumed in the calculation that *A*-site is occupied by M^{1+} and M^{2+} elements including Mn (as Mn^{2+}) and Fe^{2+}. Ferrous iron is derived as surplus Fe above the relation (Fe+Al+Ti) = 3 in *B*-site. A similar behaviour of Mn and Fe, as observed in minerals of the rockbridgeite – frondelite series (Mn is bound only as Mn^{2+}; Fe is dominantly ferric, but some ferrous iron is also present), is characteristic. Note that rockbridgeite – frondelite minerals occur in close association with ***UNK9***.

A-site in ***UNK9*** (Fig. 40) is dominated by Mn (1.16 to 1.99 *apfu*), followed by Fe^{2+} (0–0.51 *apfu*), minor Ca (0.01–0.13 *apfu*), Na (0–0.13, exceptionally 0.22 *apfu*),

Table 20 Chemical composition of ***UNK9*** (in wt. %)

	mean	1	2	3	4	5	6*
Na_2O	0.24	0.01	0.08	0.13	0.09	0.22	0.00
CaO	0.39	0.11	0.13	0.08	0.05	0.23	0.00
FeO*	2.70	1.99	0.77	1.95	2.38	0.86	0.32
BaO	0.07	0.11	0.00	0.00	0.23	0.00	0.00
MgO	0.15	0.10	0.31	0.58	0.53	0.18	0.00
PbO	0.06	0.12	0.00	0.00	0.06	0.00	0.00
CuO	0.10	0.00	0.00	0.00	0.29	0.00	0.00
MnO	17.39	18.86	20.70	17.93	18.03	19.39	21.90
ZnO	0.24	0.23	0.20	0.05	0.03	0.23	0.00
Fe_2O_3*	33.59	34.62	31.17	31.20	30.92	31.82	34.65
Al_2O_3	0.86	0.45	2.98	2.32	2.42	2.27	0.00
TiO_2	0.07	0.35	0.08	0.02	0.02	0.07	0.00
SiO_2	0.04	0.06	0.00	0.05	0.00	0.00	0.00
As_2O_5	0.06	0.09	0.22	0.09	0.14	0.00	0.00
P_2O_5	31.00	31.54	31.76	30.87	30.76	31.46	30.80
SO_3	0.03	0.04	0.03	0.00	0.03	0.06	0.00
H_2O**	8.00	8.00	8.00	8.00	8.00	8.00	8.25
total	94.99	96.68	96.42	93.26	93.97	94.79	95.92
Na^+	0.053	0.002	0.017	0.028	0.019	0.047	0.000
Ca^{2+}	0.047	0.013	0.016	0.010	0.007	0.027	0.000
Fe^{2+}	0.257	0.186	0.072	0.186	0.229	0.081	0.031
Ba^{2+}	0.003	0.005	0.000	0.000	0.010	0.000	0.000
Mg^{2+}	0.026	0.017	0.051	0.099	0.091	0.030	0.000
Pb^{2+}	0.002	0.004	0.000	0.000	0.002	0.000	0.000
Cu^{2+}	0.008	0.000	0.000	0.000	0.025	0.000	0.000
Mn^{2+}	1.678	1.786	1.947	1.736	1.752	1.846	2.134
Zn^{2+}	0.020	0.019	0.016	0.004	0.002	0.019	0.000
Σ *A*-site	2.094	2.033	2.118	2.063	2.137	2.051	2.165
Fe^{3+}	2.878	2.912	2.604	2.685	2.671	2.693	3.000
Al^{3+}	0.116	0.059	0.390	0.313	0.327	0.301	0.000
Ti^{4+}	0.006	0.029	0.006	0.002	0.001	0.006	0.000
Σ *B*-site	3.000	3.000	3.000	3.000	3.000	3.000	3.000
Si^{4+}	0.005	0.007	0.000	0.006	0.000	0.000	0.000
As^{5+}	0.004	0.005	0.013	0.005	0.008	0.000	0.000
P^{5+}	2.989	2.985	2.985	2.989	2.989	2.995	3.000
S^{6+}	0.003	0.003	0.002	0.000	0.003	0.005	0.000
Σ *T*-site	3.000	3.000	3.000	3.000	3.000	3.000	3.000
H^+	6.077	5.966	5.924	6.103	6.125	6.001	6.331
OH	4.139	4.088	4.228	4.095	4.260	4.067	4.330
H_2O	0.969	0.939	0.848	1.004	0.933	0.967	1.001

mean of all 23 spot analyses, 1–5 – representative spot analyses; 6* – unnamed mineral (dufrénite-like), Buranga, Rwanda (Knorring – Sahama, 1982). Empirical formulas were calculated on the basis of (P+As+Si+S) = 3;
*calculation of Fe_{tot} to Fe^{2+} and Fe^{3+} is based on the assumption that Fe^{3+} (jointly with Al^{3+} and Ti^{4+}) preferentially fills the B position; only Fe in surplus, above 3 *apfu,* enters the A position as Fe^{2+};
H_2O** content determined by thermal gravimetric analysis (Thermobalance TG-750 Stanton-Redcroft).

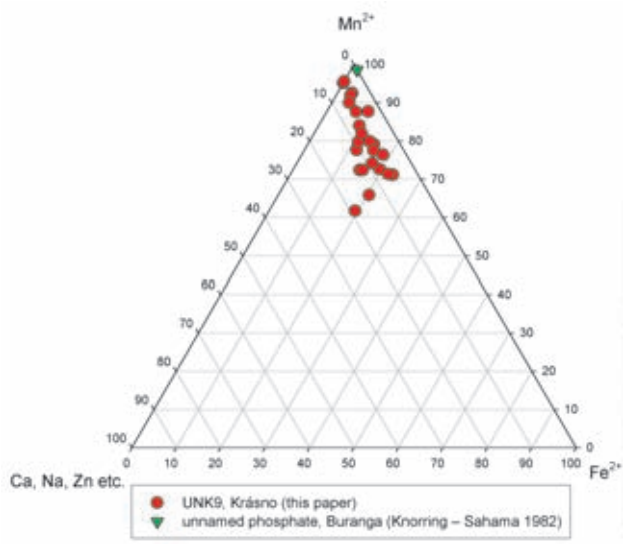

Fig. 40 Ternary plot Fe^{2+}-Mn^{2+}-(Ca+Na+Zn etc.) of *A*-site occupancy (atomic ratios) for ***UNK9*** from Krásno.

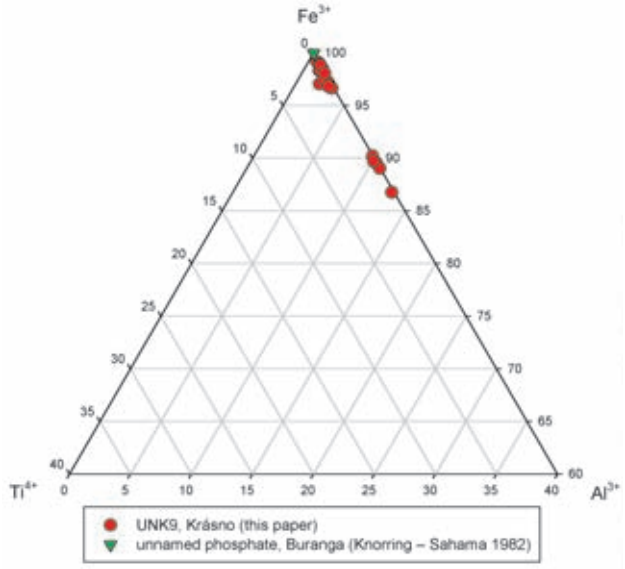

Fig. 41 Part of ternary plot Al^{3+}-Fe^{3+}-Ti^{4+} of *B*-site occupancy (atomic ratios) for ***UNK9*** from Krásno.

Cu and Zn (max. 0.04, 0.06 *apfu*, respectively), and minor Ba, Mg and Pb to 0.01 *apfu*. The total occupancy of *A*-site in ***UNK9*** is 1.76 to 2.34 *apfu*. In the *B*-site (Fig. 41) Fe^{3+} is the dominating cation ranging from 2.60 to 2.98 *apfu*. Al content is 0.02–0.12 *apfu* and 0.29–0.39 *apfu* and minor Ti to 0.03 *apfu*. Variable Al content in the *B*-site does not correlate with Mn content or other elements in *A*-site of ***UNK9***. The tetrahedral *T*-site is occupied almost exclusively by P (2.98–3.00 *apfu*), while Si is only to 0.02 *apfu*, As and S are to 0.01 *apfu* in maximum. The empirical formula for average composition (n = 23 spot analyses) of ***UNK9*** on the basis of (P+As+Si+S) = 3 is $(Mn_{1.68}Fe^{2+}_{0.26}Na_{0.05}Ca_{0.04}Mg_{0.03}Zn_{0.02})_{\Sigma 2.08}(Fe^{3+}_{2.88}Al_{0.12})_{\Sigma 3.00}(PO_4)_{2.99}(OH)_{4.14} \cdot 0.97H_2O$. The empirical formula for unnamed FeMn-phosphate from Buranga (Knorring – Sahama 1982), on the same basis as above, is $(Mn_{2.13}Fe_{0.03})_{\Sigma 2.16}Fe_{3.00}(PO_4)_{3.00}(OH)_{4.33} \cdot 1.00H_2O$.

UNK10 Fe phosphate – $(\square,Cu)Fe^{3+}_6(PO_4)_2(PO_3OH)_2(OH)_8 \cdot 4H_2O$

UNK10 has been found in a single specimen from the Huber open pit, in weathered cavities 2 by 3 cm in size, in phosphate accumulation of light pink fluorapatite and isokite with triplite relics (Sejkora *et al*. 2006c). The cav-

Fig. 42 Irregular zones of ***UNK10*** (marked by U) in zoned aggregates of the turquoise group minerals, which overgrow aggregate of *UNK3* tabular crystals (light). Aggregates of *UNK1* (tabular crystals – 1) and pharmacosiderite crystals (light – P) are present at the margin. Width of the area shown 300 μm. Cameca SX100, BSE photograph by J. Sejkora and R. Škoda.

Table 21 Chemical composition of ***UNK10*** (in wt. %)

	mean	1	2	3
CaO	0.03	0.06	0.02	0.00
BaO	0.11	0.00	0.33	0.00
PbO	0.09	0.08	0.18	0.00
CuO	2.33	1.49	2.03	3.47
MnO	0.09	0.04	0.08	0.16
ZnO	0.33	0.16	0.30	0.54
Al_2O_3	4.38	4.12	4.27	4.76
Fe_2O_3	43.41	43.44	44.19	42.60
TiO_2	0.05	0.05	0.04	0.05
SiO_2	0.04	0.04	0.06	0.03
As_2O_5	7.10	7.50	7.42	6.39
P_2O_5	25.56	25.37	25.26	26.05
SO_3	0.07	0.09	0.00	0.12
H_2O	16.64	17.09	16.38	16.51
total	100.23	99.52	100.55	100.67
Ca^{2+}	0.004	0.010	0.003	0.000
Ba^{2+}	0.007	0.000	0.020	0.000
Pb^{2+}	0.004	0.003	0.008	0.000
Cu^{2+}	0.276	0.176	0.242	0.411
Mn^{2+}	0.012	0.005	0.011	0.021
Zn^{2+}	0.039	0.019	0.035	0.063
□	0.658	0.786	0.682	0.505
Σ *A*-site	1.000	1.000	1.000	1.000
Fe_{3+}	5.135	5.127	5.253	5.026
Al^{3+}	0.811	0.761	0.794	0.879
Ti^{4+}	0.006	0.006	0.005	0.006
Σ *B*-site	5.952	5.894	6.053	5.910
Si^{4+}	0.007	0.006	0.009	0.005
As^{5+}	0.584	0.615	0.613	0.524
P^{5+}	3.401	3.369	3.378	3.457
S^{6+}	0.008	0.010	0.000	0.014
Σ *T*-site	4.000	4.000	4.000	4.000
H^+	17.448	17.880	17.261	17.266
PO_3OH	1.451	1.880	1.256	1.265
PO_4	1.950	1.489	2.122	2.192
OH	8.000	8.000	8.000	8.000
H_2O	3.999	4.000	4.002	4.001

Average composition and 1, 2, 3 – spot analyses of ***UNK10***.
Empirical formulas were calculated on the basis of (P+As+Si+S) = 4;
* H_2O content calculated from the general formula [(OH) = 8, H_2O = 4] and charge balance.

ities carry small (< 1 mm) crystalline aggregates of UNK3, overgrown by zoned minerals of the turquoise group, pharmacosiderite, UNK1, and rare kolbeckite and Cl-rich fluorapatite. During the quantitative chemical study of the zoned aggregates of turquoise group minerals, the phase has been found as several irregular zones to 20 by 50 μm in size (Fig. 42).

Owing to small dimensions of ***UNK10*** it was not possible to examine this phase by X-ray powder diffraction. Its classification with the turquoise group is based on chemical composition and its presence as zones in minerals of the turquoise group.

The quantitative chemical analyses of ***UNK10*** (Table 21) shows that it is a new mineral phase with stoichiometry corresponding to the turquoise group. The general formula of minerals of the turquoise group is $AB_6(TO_4)_{4-x}(TO_3OH)_x(OH)_8 \cdot 4H_2O$, where x = 0–2 in dependence on occupancy of the *A*-site (Foord – Taggart 1998). The *A*-site can be occupied by Cu (turquoise, chalcosiderite), Zn (faustite), Fe^{2+} (aheylite) and vacancy (planerite); *B*-site is occupied dominantly by Al and lesser Fe (chalcosiderite and unnamed Fe^{2+} – Fe^{3+} dominant member); the tetrahedral *T*-site is occupied in known members of the series always by phosphorus (Foord – Taggart 1998).

The *A*-site of ***UNK10*** contains Cu (0.17–0.41 *apfu*), Zn (0.02–0.06 *apfu*) and only minor Mn, Ba (max. 0.02 *apfu*) and Pb, Ca (max. 0.01 *apfu*). These compositional data show dominant vacancy in this position, ranging from 0.51 to 0.78 *apfu* (Fig. 43). *B*-site is dominated by Fe (5.03–5.25 *apfu*), Al corresponds to 0.76-0.88 *apfu* and Ti does not exceed 0.01 *apfu*. The tetrahedral *T*-site contains dominant P (3.37–3.46 *apfu*), regular As (0.52–

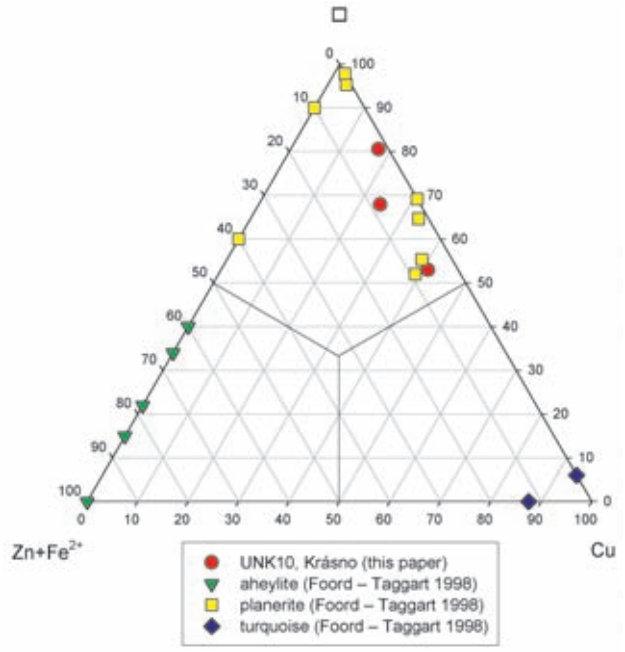

Fig. 43 Ternary plot Cu-□-(Fe^{2+}+Zn) of *A*-site occupancy (atomic ratios) for *A*-deficient members of the turquoise group.

0.62 *apfu*) and minor S and Si (max. 0.01 *apfu*). Similar contents of As in *T*-site (max. 0.60–0.64 *apfu*) were reported in minerals of the chalcosiderite – turquoise from the Huber open pit (Sejkora *et al*. 2006c) and from greisen at the Vysokém kámen quarry near Krásno (Sejkora *et al.* 2006a). The empirical formula for ***UNK10***, based on average of three spot analyses and the relationship (P+As+S+Si) = 4, is $(\square_{0.67}Cu_{0.28}Zn_{0.04}Mn_{0.01})_{\Sigma 1.00}(Fe_{5.14}Al_{0.81}Ti_{0.01})_{\Sigma 5.96}[(PO_4)_{1.95}(PO_3OH)_{1.45}(AsO_4)_{0.58}(SO_4)_{0.01}(SiO_4)_{0.01}]_{\Sigma 4.00}(OH)_{8.00} \cdot 4H_2O$.

UNK10 is the first Fe^{3+} member of the turquoise group with dominating vacancy in the *A*-site; its Al^{3+} analogue – the mineral planerite (Foord – Taggart 1998) is known for a longer time from numerous localities.

UNK11 Ca-Fe phosphate – $(Ca,Bi)(Fe,Al)_3(PO_4)(PO_3OH)(OH)_6$

UNK11 has been found in cavities in quartz in greisen samples collected behind the area of the former Stannum mine. The material originates in the Huber open pit and it was transported to the place of a secondary occurrence (Novák *et al.* 2001). ***UNK11*** in a mixture with Sr-Bi-rich crandallite occurs as light yellow-white, yellow-brown or grey aggregates among quartz crystals and mat earthy crusts up to 3 mm thick on cassiterite and quartz. Soft white dickite aggregates and thin brown-yellow or yellow coatings of *varlamoffite* (Novák *et al.* 2001) occur in a close association with ***UNK11***.

Novák *et al*. (2001) reported that *"bismutian ferricrandallite"* (i.e., the phase ***UNK11***) very closely associates with Sr-Bi crandallite and the two phases are macroscopically indistinguishable. The single additional information about this mineral phase is the following average of three spot analyses (ED analyzer; the analyses were probably normalized to 100 wt. %, fluorine was not analyzed): 14.63 Bi_2O_3, 4.07 CaO, 3.80 SrO, 1.82 CuO, 12.45 Al_2O_3, 23.43 Fe_2O_3, 16.36 P_2O_5, 11.52 As_2O_5, 2.23 SO_3, 10.17 H_2O (calculated on the basis of charge balance and (OH) = 6), total 100.48 wt. %. With regard to the general formula of the crandallite group $A^{2+,3+}B^{3+,2+}_3(TO_4)(TO_3OH)(OH)_6$, it is possible to express the empirical formula for ***UNK11*** on the basis of (P+As+S) = 2 as $(Ca_{0.40}Bi_{0.35}Sr_{0.20})_{\Sigma 0.95}(Fe_{1.64}Al_{1.36}Cu_{0.13})_{\Sigma 3.13}[(PO_4)_{0.96}(PO_3OH)_{0.32}(AsO_4)_{0.56}(SO_4)_{0.16}]_{\Sigma 2.00}(OH)_{6.00}$. Although there are high Bi, Al and As contents in individual sites, the empirical formula defines a new mineral species – Ca-Fe-P dominated member of the crandallite group (Fe analogue of crandallite or Ca analogue of zairite).

Conclusion

The complex mineralogical study in the Krásno – Horní Slavkov area, western Bohemia, Czech Republic, indicates the presence of the following eleven probably new mineral species:

UNK1 – hexagonal, $(Ca,Sr)_3Al_7(SiO_4)_3(PO_4)_3(F,OH)_3 \cdot 16.5\ H_2O$

Probably fluorine analogue of perhamite, defined on the basis of X-ray powder diffraction data, refined unit-cell parameters and quantitative chemical analyses. A mineral phase of comparable composition is not described in the available literature.

UNK2 – triclinic, $Cu_{13}(AsO_4)_6(AsO_3OH)_4 \cdot 23\ H_2O$

A Cu-arsenate that is structurally different from known minerals and synthetic materials. It is defined on the basis of X-ray powder diffraction data, refined unit-cell parameters and semi-quantitative chemical analyses. In the course of study of this phase in samples from Krásno, well-formed crystals of UNK2 have been found in samples from the Jáchymov ore district (Krušné hory Mts., Czech Republic). Results of a detailed study of these crystals, including quantitative chemical analyses and crystal structure identification based on single-crystal X-ray diffraction were submitted as a new mineral proposal to the Commission on New Minerals and Mineral names of the International Mineralogical Association. The proposal was approved under the number IMA 2004-38 as a new mineral species.

UNK3 – orthorhombic (?) – $Zn(Fe,Zn,Al)_4(PO_4)_3(OH)_4$ (?)

Probably Zn analogue of rockbridgeite and frondelite, defined on the basis of X-ray powder diffraction data, refined unit-cell parameters and quantitative analyses. No description of a mineral phase of comparable composition has been found in the literature.

UNK4 – trigonal (?),$CaAl_3(PO_4)(PO_3OH)(OH,F)_6$ (?)

Fluorine-rich Ca-Al phosphate, probably structurally related to crandallite. It was defined in mixture with fluorapatite on the basis of X-ray powder diffraction data, refined unit-cell parameters and quantitative analyses. No description of a mineral phase of comparable composition has been found in the literature.

UNK5 – $Pb(UO_2)_3O_3(OH)_2 \cdot 3H_2O$ (?)

Pb-U-oxide/hydroxide mineral without direct structural relation to known mineral species. It is defined on the basis of X-ray powder diffraction data and chemical composition, which is near to the composition of masuyite. The X-ray data indicate that this phase is identical with the unnamed mineral („$PbO\text{-}UO_3\text{-}H_2O$ phase") from Rovnost mine, Jáchymov (Ondruš *et al.* 1997).

UNK6 – monoclinic, $CuFe^{3+}_2(PO_4)_2(OH)_2 \cdot 4H_2O$

Cu, Fe^{3+}, P – dominant member of the arthurite group, P-analogue of arthurite, defined on the basis of X-ray powder diffraction data, refined unit-cell parameters and quantitative analyses.

A mineral phase from Hingston Down, Consols mine, Calstock, Cornwall (Great Britain), probably identical with UNK6, is mentioned by Frost *et al.* (2003) under the name of arthurite; however, the data by Frost *et al.* (2003) are only of a preliminary character.

UNK7 – monoclinic (?), $ZnFe^{3+}_2(PO_4)_2(OH)_2 \cdot 4H_2O$

Zn, Fe^{3+}, P – dominated member of the arthurite group, P-analogue of ojuelaite, has been defined on the

basis of chemical analyses. No description of a mineral phase of comparable composition has been found in the literature.

UNK8 – monoclinic (?), $Fe^{2+}Al_2(PO_4)_2(OH)_2 \cdot 4H_2O$

Fe^{2+}, Al^{3+}, P – dominant member of the arthurite group, Al-analogue of whitmoreite, defined only on the basis of chemical analyses. No description of a mineral phase of comparable composition has been found in the literature.

UNK9 – monoclinic, $(Mn^{2+},Fe^{2+})_2(Fe^{3+},Al)_3(PO_4)_3(OH)_4 \cdot H_2O$

Fe-Mn phosphate, unrelated to compounds of a similar composition. It is defined on the basis of X-ray powder diffraction data and quantitative chemical analyses. The phase is probably identical with unnamed "dufrénite-like" mineral from Buranga (Knorring – Sahama 1982) and related to (Mn analogue of ?) an unnamed Fe phosphate from Rothläufchen mine, Waldgirmes (Frondel 1949).

UNK10 – triclinic (?), $(\square,Cu)Fe^{3+}_6(PO_4)_2(PO_3OH)_2(OH)_8 \cdot 4H_2O$

□, Fe^{3+}, P – dominant member of the turquoise group, Fe^{3+}-analogue of planerite, defined only on the basis of quantitative chemical analyses. No description of a mineral phase of comparable composition has been found in the literature.

UNK11 – trigonal(?), $(Ca,Bi)(Fe,Al)_3(PO_4)(PO_3OH)(OH)_6$

Ca, Fe^{3+}, P – dominated member of the crandallite group, Ca-analogue of zairite or Fe^{3+}-analogue of crandallite, defined only on the basis of quantitative chemical composition. No description of a mineral phase of comparable composition has been found in the literature.

Acknowledgements. The authors gratefully acknowledge cooperation of Jiří Litochleb, Jiří Čejka (National Museum, Prague), Stanislav Vrána, František Veselovský, Ananda Gabašová (Czech Geological Survey, Prague), Jakub Plášil, Pavel Škácha (Faculty of Science, Charles University, Prague), Jana Ederová (Institute of Chemical Technology, Prague) and numerous colleagues who kindly provided samples for this study – Ctibor Süsser (Sokolov), Jaromír Tvrdý (Karlovy Vary), Pavel Beran (Sokolov) and others.

This work was supported by Grants from the Ministry of Culture of the Czech Republic (Project MK00002327201) and the Granting Agency of the Czech Republic (Grant No. 205/03/D004).

Submitted September 9, 2006

References

Beran, P. – Sejkora, J. (2006): The Krásno Sn-W ore district near Horní Slavkov: mining history, topographical, geological and mineralogical characteristics. – Journ. Czech Geol. Soc., 51: 3–42

Blount, A. M. (1974): The crystal structure of crandallite. – Amer. Mineral., 59: 41–47.

Burnham, C. W. (1962): Lattice constant refinement. Carnegie Inst. Washington Year Book 61: 132–135.

Burns, P. C. (1997): A new uranyl oxide hydrate sheet in vandendriesscheite: Implication fro mineral paragenesis and the corrosion of spent nuclear fuel. – Amer. Mineral., 82, 1176–1186.

– (1998): The structure of richetite, a rare lead uranyl oxide hydrate. – Can. Mineral., 36: 187–199.

Burns, P. C. – Hanchar, J. M. (1999): The structure of masuyite, $Pb[(UO_2)_3O_3(OH)_2]((H_2O)_3$, and its relationship to protasite. – Can. Mineral., 37: 1483–1491.

Cesbron, F. – Romero, M. – Williams, S. A. (1981): La mapimite et l'ojuelaite, deux nouveaux arséniates hydratés de zinc et de fer de la mine Ojuela, Mapimi, Mexique. – Bull. Minéral., 104: 582–586.

Christ, C. L. – Clark, J. R. (1960): Crystal chemical studies of some uranyl oxide hydrates. – Amer. Mineral., 45, 1026–1061.

Cowgill, U. M. – Hutchinson, G. E. – Joensuu, O. (1963): An apparently triclinic dimorph of crandallite from a tropical swamp sediment in El Petén, Guatemala. – Amer. Mineral., 48: 1144–1153.

Davis, R. J. – Hey, M. H. (1964): Arthurite, a new copper-iron arsenate from Cornwall. – Mineral. Mag. 33, 937–941

– (1969): The cell-contents of arthurite redetermined. – Mineral. Mag., 37, 520–521.

Deliens, M. – Piret, P. (1996): Les Masuyites de Shinkolobwe (Shaba, Zaďre) constituent un groupe formé de deux variétés distinctes par leur composition chimique et leurs propriétés radiocristallographiques. – Bull. Inst. Roayl Scinces Natur. Belgique, Sciences de la Terre, 66: 187–192.

Dunn, P. J. – Appleman, D. E. (1977): Perhamite, a new calcium aluminum silico-phosphate mineral, and a re-examination of viséite. – Mineral. Mag. 41: 437–442.

Finch, R. J. – Ewing, R. C. (1992): The corrosion of uraninite under oxidizing conditions. – Journ. Nucl. Mater., 190: 133–156.

Foord, E. E. – Taggart, J. E. Jr. (1998): A re-examination of the turquoise group: the mineral aheylite, planerite (redefined), turquoise and coeruleolactite. – Mineral. Mag. 62: 93–111.

Frondel, C. (1949): The dufrenite problem. – Am. Mineral., 34: 513–539.

Frost, R. L. – Duong, L. – Martens, W. (2003): Molecular assembly in secondary minerals – Raman spectroscopy of the arthurite group species arthurite and whitmoreite. – N. Jb. Miner. Mn., 223–240.

Hughes, J. M. – Bloodaxe, E. S. – Kobel, K. D. – Drexler, J. W. (1996): The atomic arrangment of ojuelaite, $ZnFe^{3+}_2(AsO_4)_2(OH)_2 \cdot 4H_2O$. – Mineral. Mag., 60, 519–521.

Jambor, J. L. – Vinalas, J. – Groat, L. A. – Raudsepp, M. (2002): Cobaltarthurite, $Co^{2+}Fe^{3+}_2(AsO_4)_2(OH)_2 \cdot 4 H_2O$. a new member of the arthurite group. – Can. Mineral., 40, 725–732.

Kampf, A. R. (2005): The crystal structure of cobaltarthurite from the Bou Azzer district, Morocco: the location of hydrogen atoms in the arthurite structure-type. – Can. Mineral., 43: 1387–1391.

Keller, P. – Hess, H. (1978): Die Kristallstruktur von Arthurit, $CuFe^{3+}_2[(H_2O)_4|(OH)_2|(AsO_4)_2]$. – N. Jb. Miner. Abh., 133: 291–302.

Knorring v., O. – Sahama, T. G. (1982): Some FeMn phosphates from the Buranga pegmatite, Rwanda. – Schweiz. mineral. petrogr. Mitt., 62: 343–352

Li, Y. – Burns, P. C. (2000a): Investigations of crystal chemistry variability in lead uranyl oxide hydrates. II. Fourmarierite. – Can. Mineral.; 38, 797–749.

– (2000b): Synthesis and crystal structure of a new Pb uranyl oxide hydrate with a framework structure that contains channels. – Can. Mineral., 38: 1433–1441.

Mills, S. J. – Frost, R. L. – Grey, I. E. – Mumme, W. G. – Weier, M. L. (2004): Crystallography, Raman and IR spectroscopy of perhamite – an interesting silico-phosphate. – Mitt. Österr. Miner. Ges., 149: 68.

Moore, P. B. (1970): Crystal chemistry of the basic iron phosphates. – Amer. Mineral. 55: 135–169.

Moore, P. B. – Kampf, A. R. – Irving, A. J. (1974): Whitmoreite. $Fe^{2+}Fe^{3+}_2(OH)_2(H_2O)_4[PO_4]_2$, a new species: its description and atomic arrangement. – Am. Mineral., 59: 900–905.

Novák, F. – Pauliš, P. – Süsser, C. (2001): Chemical composition of crandallite, goyazite and waylandite from Krásno near Horní Slavkov. – Chemické složení crandallitu, goyazitu a waylanditu z Krásna

u Horního Slavkova. – Bull. mineral. – petrolog. Odd. Nár. Muz. (Praha), 9: 230–234. (in Czech)

Ondruš, P. (1993): ZDS – A computer program for analysis of X-ray powder diffraction patterns. – Materials Science Forum, 133–136: 297–300, EPDIC-2. Enchede.

Ondruš, P. – Skála, R. (1997): New quasi-empirical channel Search/Match algorithm for ICDD PDF2 Database: A tool for qualitative phase analysis integrated in the ZDS-System software package for X-ray powder diffraction analysis – Fifth European Powder Diffraction Conference EPDIC-5, 193. Parma.

Ondruš, P. – Veselovský, F. – Skála, R. – Císařová, I. – Hloušek, J. – Frýda, J. – Vavřin, I. – Čejka, J. – Gabašová, A. (1997): New naturally occurring phases of secondary origin from Jáchymov (Joachimsthal). – Jour. Czech Geol. Soc., 42: 77–107.

Pagoaga, M. K. (1983): The crystal chemistry of the uranyl oxide hydrate minerals. – PhD Thesis, University of Maryland.

Peacor, D. R. – Dunn, P. J. – Simmons, W. B. (1984): Earlshannonite, the Mn analogue of whitmoreite, from North Carolina. – Can. Mineral., 22: 471–474.

Pilkington, E. S. – Segnit, E. R. – Watts, J. – Francis, G. (1979): Kleemanite, a new zinc aluminium phosphate. – Mineral. Mag., 43, 93–95.

Piret, P. (1985): Structure cristalline de la fourmarierite, $Pb(UO_2)_4O_3(OH)_4 . 4 H_2O$. – Bull. Minéral., 108, 659–665.

Piret, P. – Deliens, M. – Piret-Meunier, J. – Germain, G. (1983): La sayrite, $Pb_2[(UO_2)_5O_6(OH)_2] . 4H_2O$, nouveau minéral; properiétés et structure cristalline. – Bull. minéral., 106: 299–304.

Piret, P. – Deliens, M. (1984): Nouvelles données sur la richetite $PbO.4UO_3.4H_2O$. – Bull. Minéral., 107: 581–585.

Plášil, J. – Sejkora, J. – Ondruš, P. – Veselovský, F. – Beran, P. – Goliáš, V. (2006): Supergene minerals in the Horní Slavkov uranium ore district, Czech Republic. – Journ. Czech Geol. Soc., 51: 149–158.

Pouchou, J. L. – Pichoir, F. (1985): "PAP" procedure for improved quantitative microanalysis. – Microbeam Analysis 20:104–105.

Raudsep, M. (1995): Recent advances in the electron-probe analysis of minerals for the light elements. – Canad. Mineral., 33: 203–218.

Rodríguez-Carvajal, J. (2005): Computer Program FullProf, ver. December 2005. – Laboratoire Leon Bril-louin (CEA-CNRS), France.

Sejkora, J. – Ondruš, P. – Fikar, M. – Veselovský, F. – Mach, Z. – Gabašová, A. (2006a): New data on mineralogy of the Vysoký Kámen deposits near Krásno, Slavkovský les area, Czech Republic. – Journ. Czech Geol. Soc., 51: 43–55.

Sejkora, J. – Ondruš, P. – Fikar, M. – Veselovský, F. – Mach, Z. – Gabašová, A. – Škoda, R. – Beran, P. (2006b): Supergene minerals at the Huber stock and Schnöd stock deposits, Krásno ore district, the Slavkovský les area, Czech Republic. – Journ. Czech Geol. Soc., 51: 57–101.

Sejkora, J. – Škoda, R. – Ondruš, P. – Beran, P. – Süsser, C. (2006c): Mineralogy of phosphate accumulations in the Huber stock, Krásno ore district, Slavkovský les area, Czech Republic. – Journ. Czech Geol. Soc., 51: 103–147.

Staněk, J. (1988): Paulkerrite and earlshannonite from pegmatite near Dolní Bory (western Moravia, Czechoslovakia). – Čas. Morav. Muz., Vědy přír., 73: 29–34.

Nové minerální fáze z oblasti Krásno – Horní Slavkov, západní Čechy, Česká republika

V práci je popsáno jedenáct pravděpodobně nových minerálních druhů, pocházejících z oblasti Krásno – Horní Slavkov, západní Čechy, Česká republika. Mezi zjištěnými novými druhy převažují supergenní fosfáty, dále byl zjištěn i jeden arsenát a hydroxid Pb-U. Podány jsou všechna dostupná fyzikální a chemická data pro jednotlivé zjištěné nové minerální druhy, stejně jako citace související literatury.